

$B \rightarrow K K^*$ Decays in the Perturbative QCD Approach

Libo Guo,^{*} Qian-gui Xu, and Zhen-jun Xiao[†]

*Department of Physics and Institute of Theoretical Physics,
Nanjing Normal University, Nanjing, Jiangsu 210097, P.R.China*

(Dated: October 16, 2018)

Abstract

We calculate the branching ratios and CP-violating asymmetries for $B^0 \rightarrow K^0 \bar{K}^{*0}$, $\bar{K}^0 K^{*0}$, $K^+ K^{*-}$, $K^- K^{*+}$, and $B^+ \rightarrow K^+ \bar{K}^{*0}$ and $\bar{K}^0 K^{*+}$ decays by employing the low energy effective Hamiltonian and the perturbative QCD (pQCD) factorization approach. The theoretical predictions for the branching ratios are $Br(B^0/\bar{B}^0 \rightarrow K^\pm K^{*\mp}) \approx 7.4 \times 10^{-8}$, $Br(B^0/\bar{B}^0 \rightarrow K^0 \bar{K}^{*0} (\bar{K}^0 K^{*0})) \approx 19.6 \times 10^{-7}$, $Br(B^+ \rightarrow K^+ \bar{K}^{*0}) \approx 3 \times 10^{-7}$ and $Br(B^+ \rightarrow K^{*+} \bar{K}^0) \approx 18.3 \times 10^{-7}$, which are consistent with currently available experimental upper limits. We also predict large CP-violating asymmetries in these decays: $A_{CP}^{dir}(K^\pm \bar{K}^{*0}) \approx -20\%$, $A_{CP}^{dir}(K^{*+} \bar{K}^0) \approx -49\%$, which can be tested by the forthcoming B meson experiments.

PACS numbers: 13.25.Hw, 12.38.Bx, 14.40.Aq, 14.40.Ev

arXiv:hep-ph/0609005v2 7 Dec 2006

^{*}Electronic address: guolib@njnu.edu.cn

[†]Electronic address: xiaozhenjun@njnu.edu.cn

I. INTRODUCTION

The study of exclusive non-leptonic weak decays of B mesons provides not only good opportunities for testing the Standard Model (SM) but also powerful means for probing different new physics scenarios beyond the SM. The mechanism of two body B decay is still not quite clear, although many scientists devote to this field. Starting from factorization hypothesis [1], many approaches have been built to explain the existing data and some progresses have been made. For example the generalized factorization (GF)[2], QCD factorization (QCDF) approach [3, 4], the perturbative QCD (pQCD) approach [5, 6, 7, 8] and the soft-collinear effective theory (SCET) [9]. The pQCD approach is based on K_T factorization theorem[10] while others are mostly based on collinear factorization [11].

In our opinion, the pQCD factorization approach has three special features: (a) Sudakov factor and threshold resummation [12] are included to regulate the end-point singularities, so the arbitrary cutoff[13] is no longer necessary; (b) the form factors for $B \rightarrow M$ transition can be calculated perturbatively, although some controversies still exist about this point; and (c) the annihilation diagrams are calculable and play an important role in producing CP violation [8, 14]. Up to now, many B meson decay channels have been studied by employing the pQCD approach, and it has become one of the most popular methods to calculate the hadronic matrix elements.

In this paper, we will study the branching ratios and CP asymmetries of $B \rightarrow K K^*$ decays in the pQCD factorization approach. Theoretically, in the $B \rightarrow K K^*$ decay modes, the B meson is heavy and sitting at rest. It decays into two light mesons with large momenta, so these two energetic final state mesons may have no enough time to get involved in soft final state interaction (FSI). In this case, the short distance hard process dominates the decay amplitude and the non-perturbative FSI effects may not be important, this makes the pQCD approach applicable. At the same time, the $B \rightarrow K K^*$ decays have been studied before in the GF approach [2] and the QCDF approach [3, 4]. The similar decays such as $B \rightarrow KK$ and K^*K^* decays have been investigated in the pQCD approach recently [15, 16]. On the experimental side, the first measurement of $B^0 \rightarrow (K^0\bar{K}^{*0} + \bar{K}^0 K^{*0})$ decay has been reported very recently by BaBar collaboration [17] in units of 10^{-6} (upper limits at 90% C.L.):

$$Br(B^0 \rightarrow K^0\bar{K}^{*0} + \bar{K}^0 K^{*0}) = 0.2_{-0.8-0.3}^{+0.9+0.1} (< 1.9). \quad (1)$$

For $B^+ \rightarrow K^+\bar{K}^{*0}$ decay, only the experimental upper limit is available now [18, 19]

$$Br(B^+ \rightarrow K^+\bar{K}^{*0}) < 5.3 \times 10^{-6}. \quad (2)$$

This paper is organized as follows. In Sec. II, we give the theoretical framework of the pQCD factorization approach. Next, we calculate the relevant Feynman diagrams and present the various decay amplitudes for $B \rightarrow K K^*$ decays. In Sec. IV, we show the numerical results of the CP-averaged branching ratios and CP asymmetries and compare them with currently available experimental measurements or the theoretical predictions in QCDF approach. The summary and some discussions are included in the final section.

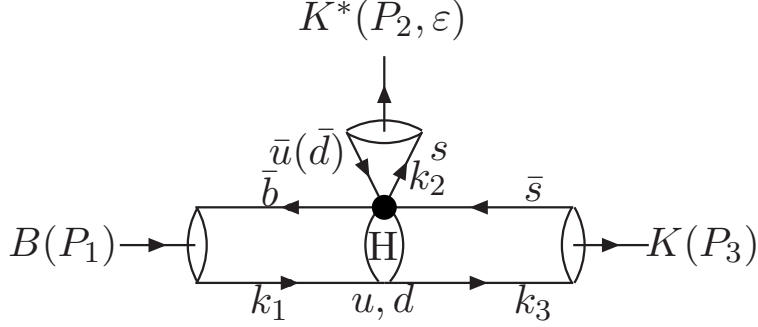


FIG. 1: Factorization for $B \rightarrow KK^*$ Decays

II. THEORETICAL FRAMEWORK

The three scales pQCD factorization approach[6, 7] has been developed and applied in the non-leptonic B meson decays for some time. In this approach, the decay amplitude is factorized into the convolution of the mesons' light-cone wave functions, the hard scattering kernel and the Wilson coefficients, as illustrated schematically by Fig. 1, which stands for the soft, hard and harder dynamics characterized by three different energy scales ($t \sim \mathcal{O}(\sqrt{\bar{\Lambda}M_B})$, m_b , M_W) respectively. Then the decay amplitude $\mathcal{A}(B \rightarrow M_1M_2)$ is conceptually written as the convolution

$$\mathcal{A}(B \rightarrow M_1M_2) \sim \int d^4k_1 d^4k_2 d^4k_3 \text{Tr} [C(t)\Phi_B(k_1)\Phi_{M_1}(k_2)\Phi_{M_2}(k_3)H(k_1, k_2, k_3, t)], \quad (3)$$

where k_i 's are momenta of light quarks included in each mesons, and the term “Tr” denotes the trace over Dirac and color indices. $C(t)$ is the Wilson coefficient which results from the radiative corrections at short distance. In the above convolution, $C(t)$ includes the harder dynamics at scale larger than M_B and describes the evolution of local 4-Fermi operators from m_W (the W boson mass) down to $t \sim \mathcal{O}(\sqrt{\bar{\Lambda}M_B})$ scale, where $\bar{\Lambda} \equiv M_B - m_b$. The function $H(k_1, k_2, k_3, t)$ describes the four quark operator and the spectator quark connected by a hard gluon whose q^2 is of the order of $\bar{\Lambda}M_B$, and includes the $\mathcal{O}(\sqrt{\bar{\Lambda}M_B})$ hard dynamics. Therefore, this hard part H can be evaluated as an expansion in power of $\alpha_S(t)$ and $\bar{\Lambda}/t$, and depends on the processes considered. The function Φ_M ($M = B, M_1, M_2$) is the wave function which describes hadronization of the quark and anti-quark into the meson M , and independent of the specific processes. Using the wave functions determined from other well measured processes, one can make quantitative predictions here.

Since the b quark is rather heavy we consider the B meson at rest for simplicity. It is convenient to use light-cone coordinate (p^+, p^-, \mathbf{p}_T) to describe the meson's momenta,

$$p^\pm = \frac{1}{\sqrt{2}}(p^0 \pm p^3), \quad \text{and} \quad \mathbf{p}_T = (p^1, p^2). \quad (4)$$

Using the light-cone coordinates the B meson and the two final state meson momenta can be written as

$$P_1 = \frac{M_B}{\sqrt{2}}(1, 1, \mathbf{0}_T), \quad P_2 = \frac{M_B}{\sqrt{2}}(1, r_{k^*}^2, \mathbf{0}_T), \quad P_3 = \frac{M_B}{\sqrt{2}}(0, 1 - r_{k^*}^2, \mathbf{0}_T), \quad (5)$$

respectively, where $r_{K^*} = m_{K^*}/m_B$; and the terms proportional to $m_{K^*}^2/m_B^2$ have been neglected.

For the $B \rightarrow KK^*$ decays considered here, only the K^* meson's longitudinal part contributes to the decays, its polarization vector is $\epsilon_L = \frac{M_B}{\sqrt{2}M_{K^*}}(1, -r_{K^*}^2, \mathbf{0}_T)$. Putting the light (anti-) quark momenta in B , K^* and K mesons as k_1 , k_2 , and k_3 , respectively, we can choose

$$k_1 = (x_1 P_1^+, 0, \mathbf{k}_{1T}), \quad k_2 = (x_2 P_2^+, 0, \mathbf{k}_{2T}), \quad k_3 = (0, x_3 P_3^-, \mathbf{k}_{3T}). \quad (6)$$

Then the integration over k_1^- , k_2^- , and k_3^+ in Eq.(3) will lead to

$$\mathcal{A}(B \rightarrow KK^*) \sim \int dx_1 dx_2 dx_3 b_1 db_1 b_2 db_2 b_3 db_3 \text{Tr} [C(t)\Phi_B(x_1, b_1)\Phi_{K^*}(x_2, b_2)\Phi_K(x_3, b_3)H(x_i, b_i, t)S_t(x_i) e^{-S(t)}], \quad (7)$$

where b_i is the conjugate space coordinate of k_{iT} , and t is the largest energy scale in function $H(x_i, b_i, t)$. The large logarithms $\ln(m_W/t)$ coming from QCD radiative corrections to four quark operators are included in the Wilson coefficients $C(t)$. The large double logarithms ($\ln^2 x_i$) on the longitudinal direction are summed by the threshold resummation[12], and they lead to $S_t(x_i)$ which smears the end-point singularities on x_i . The last term, $e^{-S(t)}$, is the Sudakov form factor resulting from overlap of soft and collinear divergences, which suppresses the soft dynamics effectively[20]. Thus it makes the perturbative calculation of the hard part H applicable at intermediate scale, i.e., M_B scale.

The weak effective Hamiltonian H_{eff} for $B \rightarrow KK^*$ decays can be written as [21]

$$\mathcal{H}_{eff} = \frac{G_F}{\sqrt{2}} \left[V_{ub}V_{ud}^* (C_1(\mu)O_1^u(\mu) + C_2(\mu)O_2^u(\mu)) - V_{tb}V_{td}^* \sum_{i=3}^{10} C_i(\mu) O_i(\mu) \right]. \quad (8)$$

where $C_i(\mu)$ are Wilson coefficients evaluated at the renormalization scale μ and O_i are the four-fermion operators for $b \rightarrow d$ transition:

$$\begin{aligned} O_1^u &= \bar{d}_\alpha \gamma^\mu L u_\beta \cdot \bar{u}_\beta \gamma_\mu L b_\alpha, & O_2^u &= \bar{d}_\alpha \gamma^\mu L u_\alpha \cdot \bar{u}_\beta \gamma_\mu L b_\beta, \\ O_3 &= \bar{d}_\alpha \gamma^\mu L b_\alpha \cdot \sum_{q'} \bar{q}'_\beta \gamma_\mu L q'_\beta, & O_4 &= \bar{d}_\alpha \gamma^\mu L b_\beta \cdot \sum_{q'} \bar{q}'_\beta \gamma_\mu L q'_\alpha, \\ O_5 &= \bar{d}_\alpha \gamma^\mu L b_\alpha \cdot \sum_{q'} \bar{q}'_\beta \gamma_\mu R q'_\beta, & O_6 &= \bar{d}_\alpha \gamma^\mu L b_\beta \cdot \sum_{q'} \bar{q}'_\beta \gamma_\mu R q'_\alpha, \\ O_7 &= \frac{3}{2} \bar{d}_\alpha \gamma^\mu L b_\alpha \cdot \sum_{q'} e_{q'} \bar{q}'_\beta \gamma_\mu R q'_\beta, & O_8 &= \frac{3}{2} \bar{d}_\alpha \gamma^\mu L b_\beta \cdot \sum_{q'} e_{q'} \bar{q}'_\beta \gamma_\mu R q'_\alpha, \\ O_9 &= \frac{3}{2} \bar{d}_\alpha \gamma^\mu L b_\alpha \cdot \sum_{q'} e_{q'} \bar{q}'_\beta \gamma_\mu L q'_\beta, & O_{10} &= \frac{3}{2} \bar{d}_\alpha \gamma^\mu L b_\beta \cdot \sum_{q'} e_{q'} \bar{q}'_\beta \gamma_\mu L q'_\alpha, \end{aligned} \quad (9)$$

where α and β are the $SU(3)$ color indices; L and R are the left- and right-handed projection operators with $L = (1 - \gamma_5)$, $R = (1 + \gamma_5)$. The sum over q' runs over the quark fields that are active at the scale $\mu = O(m_b)$, i.e., ($q' \in \{u, d, s, c, b\}$). For the decays with $b \rightarrow s$ transition, simply make a replacement of d by s in Eqs. (8) and (9).

The pQCD approach works well for the leading twist approximation and leading double logarithm summation. For the Wilson coefficients $C_i(\mu)$ ($i = 1, \dots, 10$), we will also use the leading order (LO) expressions, although the next-to-leading order calculations already exist in the literature [21]. This is the consistent way to cancel the explicit μ dependence in the theoretical formulae. For the renormalization group evolution of the

Wilson coefficients from higher scale to lower scale, we use the leading logarithmic running equations as given in Appendix C and D of Ref. [22].

In the resummation procedures, the B meson is treated as a heavy-light system. In general, the B meson light-cone matrix element can be decomposed as [23]

$$\begin{aligned} & \int_0^1 \frac{d^4 z}{(2\pi)^4} e^{i\mathbf{k}_1 \cdot \mathbf{z}} \langle 0 | \bar{b}_\alpha(0) d_\beta(z) | B(p_B) \rangle \\ &= -\frac{i}{\sqrt{2N_c}} \left\{ (\not{p}_B + m_B) \gamma_5 \left[\phi_B(\mathbf{k}_1) - \frac{\not{n}_+ - \not{n}_-}{\sqrt{2}} \bar{\phi}_B(\mathbf{k}_1) \right] \right\}_{\beta\alpha}, \end{aligned} \quad (10)$$

where $n_+ = (1, 0, \mathbf{0}_T)$, and $n_- = (0, 1, \mathbf{0}_T)$ are the unit vectors pointing to the plus and minus directions, respectively. From the above equation, one can see that there are two Lorentz structures in the B meson distribution amplitudes. They obey to the following normalization conditions

$$\int \frac{d^4 k_1}{(2\pi)^4} \phi_B(\mathbf{k}_1) = \frac{f_B}{2\sqrt{2N_c}}, \quad \int \frac{d^4 k_1}{(2\pi)^4} \bar{\phi}_B(\mathbf{k}_1) = 0. \quad (11)$$

In general, one should consider these two Lorentz structures in calculations of B meson decays. However, it can be argued that the contribution of $\bar{\phi}_B$ is numerically small [24], thus its contribution can be numerically neglected safely. Using this approximation, we can reduce one input parameter in our calculation. Therefore, we only consider the contribution of Lorentz structure

$$\Phi_B = \frac{1}{\sqrt{2N_c}} (\not{p}_B + m_B) \gamma_5 \phi_B(\mathbf{k}_1). \quad (12)$$

The K and K^* mesons are treated as a light-light system. Based on the $SU(3)$ flavor symmetry, we assume that the wave functions of K and K^* mesons are the same in structure as the wave functions of π and ρ , respectively, then the K meson wave function is defined as [25, 26]

$$\Phi_K(P, x, \zeta) \equiv \frac{1}{\sqrt{2N_c}} \gamma_5 \{ \not{p} \phi_K^A(x) + m_0^K \phi_K^P(x) + \zeta m_0^K (\not{p} \not{n} - v \cdot n) \phi_K^T(x) \} \quad (13)$$

where P and x are the momentum and the momentum fraction of K , respectively. The parameter ζ is either $+1$ or -1 depending on the assignment of the momentum fraction x . While in $B \rightarrow KK^*$ decays, K^* meson is longitudinally polarized, only the longitudinal component $\Phi_{K^*}^L$ of the wave function should be considered [24, 27],

$$\Phi_{K^*}^L = \frac{1}{\sqrt{2N_c}} \{ \not{\epsilon} [\not{p} \phi_{K^*}^T(x) + m_{K^*} \phi_{K^*}(x)] + m_{K^*} \phi_{K^*}^S(x) \}. \quad (14)$$

The second term in above equation is the leading twist wave function (twist-2), while the first and third terms are sub-leading twist (twist-3) wave functions. The transverse part of Φ_{K^*} can be found for example in Ref. [16].

The explicit expressions of the distribution functions $\phi_B(\mathbf{k}_1)$, $\phi_K^A(x)$, $\phi_K^P(x)$, $\phi_K^T(x)$, $\phi_{K^*}(x)$, $\phi_{K^*}^S(x)$ and $\phi_{K^*}^T(x)$ will be given in next section. The initial conditions of leading

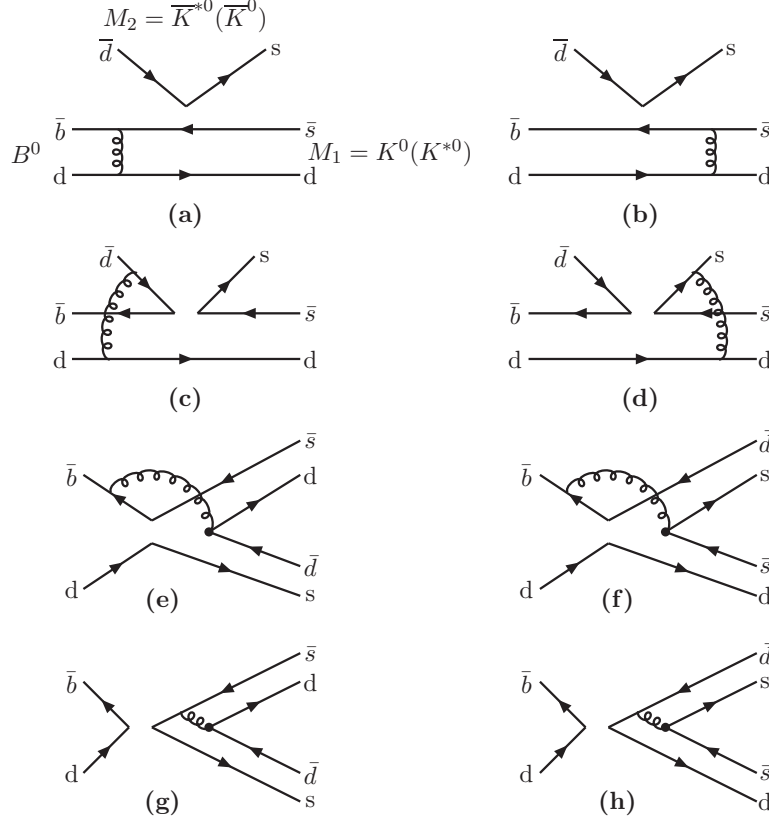


FIG. 2: Typical Feynman diagrams contributing to $B^0 \rightarrow K^0 \bar{K}^{*0} (K^{*0} \bar{K}^0)$ decays. The diagram (a) and (b) contribute to the form factor $A_0^{B \rightarrow K^*}$ or $F_{0,1}^{B \rightarrow K}$ for $M_1 = K^{*0}$ or K^0 , respectively. Other four Feynman diagrams obtained by connecting the gluon lines to the d quark line inside the B^0 meson for (e) and (f), and to the lower s or d quark line for (g) and (h) are omitted.

twist distribution functions $\phi_i(x)$, $i = B, K^*, K$, are of non-perturbative origin, satisfying the normalization condition

$$\int_0^1 \phi_i(x, b=0) dx = \frac{1}{2\sqrt{6}} f_i, \quad (15)$$

where f_i is the decay constant of the corresponding meson.

III. PERTURBATIVE CALCULATIONS

For the considered decay modes, the Feynman diagrams are shown in Figs. 2-4. We firstly analyze the corresponding decay modes topologically: (i) the eight diagrams can be categorized into emission and annihilation diagrams; (ii) each category contains four diagrams: two factorizable and two nonfactorizable. In Fig. 2, for example, Figs. 2(a-d) are emission diagrams, while Figs. 2(e-h) are annihilation ones topologically; and Figs. 2(a,b,g,h) are factorizable and Figs. 2(c-f) are nonfactorizable diagrams.

For $B^0 \rightarrow K^0 \bar{K}^{*0} (K^{*0} \bar{K}^0)$ decays, only the operators O_{3-10} contribute via penguin topology with light quark $q = s$ (diagrams a,b,c,d) and via the annihilation topology with the light quark $q = d$ (diagram 2(f) and 2(h)) or s (diagram 2(e) and 2(g)). It is

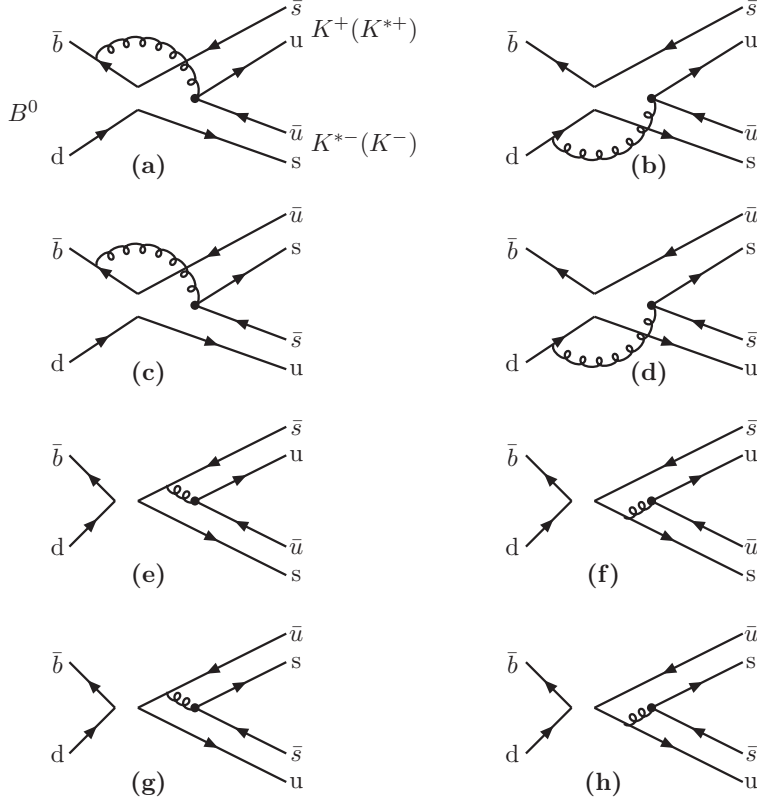


FIG. 3: Feynman diagrams for $B^0 \rightarrow K^+ K^{*-} (K^{*+} K^-)$ decays.

a pure penguin mode with only one kind of CKM elements, and consequently, there is no CP violation for these decays.

For the $B^0(\bar{B}^0) \rightarrow K^+ K^{*-} (K^{*+} K^-)$ decays (see Fig. 3), the current-current operators $O_{1,2}^{(u)}$ contribute via the annihilation topology (Figs. 3(c,d,g,h)), while the operators O_{3-10} contribute via the annihilation topology with the light quark $q = s$ (Figs. 3(a,b,e,f)) or $q = u$ (Figs. 3(c,d,g,h)).

For the $B^+ \rightarrow K^+ \bar{K}^{*0} (K^{*+} \bar{K}^0)$ decays (see Fig. 4), the current-current operators $O_{1,2}^{(u)}$ contribute via the annihilation topology (Figs. 4(e-h)), while the penguin operators O_{3-10} contribute via the penguin topology with the light quark $q = s$ (Figs. 4(a-d)) or via the annihilation topology with $q = u$ (Figs. 4(e-h)).

In the analytic calculations, the operators with $(V - A)(V - A)$ structure work directly, while the operators with $(V - A)(V + A)$ structure will work in two different ways:

- In some decay channels, some of these operators contribute directly to the decay amplitude in a factorizable way.
- In some other cases, we need to do Fierz transformation for these operators to get right flavor and color structure for factorization to work. In this case, we get $(S + P)(S - P)$ operators from $(V - A)(V + A)$ ones.

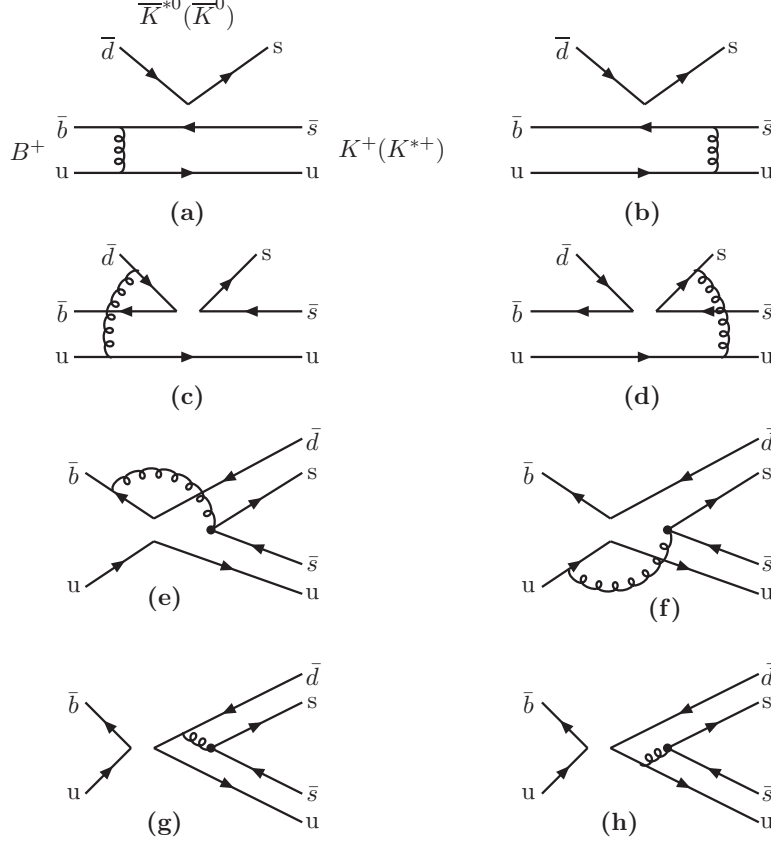


FIG. 4: Feynman diagrams for $B^+ \rightarrow K^+ \bar{K}^{*0} (K^{*+} \bar{K}^0)$ decays.

A. $B^0 \rightarrow K^0 \bar{K}^{*0} (K^{*0} \bar{K}^0)$ decay

For the sake of the reader, we take the $B^0 \rightarrow K^0 \bar{K}^{*0} (K^{*0} \bar{K}^0)$ decay channel as an example to show the ways to derive the decay amplitude from individual diagram. As shown explicitly in Fig. 2(a), the meson M_1 which picks up the spectator quark can be K^0 or K^{*0} , the emitted meson M_2 should be \bar{K}^{*0} or \bar{K}^0 at the same time. The B^0 meson therefore can decay into the final state $f = K^0 \bar{K}^{*0}$ and $\bar{f} = K^{*0} \bar{K}^0$ simultaneously. The \bar{B}^0 meson, on the other hand, also decay into the same final state $f = K^0 \bar{K}^{*0}$ and $\bar{f} = K^{*0} \bar{K}^0$ simultaneously.

Now we consider the usual factorizable diagram 2(a) and 2(b) for the case of $M_1 = K^{*0}$. The $(V - A)(V - A)$ operators $O_{3,4}$ and $O_{9,10}$ contribute through diagram 2(a) and 2(b), the sum of their contributions is given as

$$\begin{aligned}
F_{eK^*} = & 4\sqrt{2}G_F\pi C_F f_K m_B^4 \int_0^1 dx_1 dx_3 \int_0^\infty b_1 db_1 b_3 db_3 \phi_B(x_1, b_1) \\
& \cdot \{ [(1+x_3)\phi_{K^*}(x_3, b_3) + (1-2x_3)r_{K^*}(\phi_{K^*}^s(x_3, b_3) + \phi_{K^*}^t(x_3, b_3))] \\
& \cdot \alpha_s(t_e^1) h_e(x_1, x_3, b_1, b_3) \exp[-S_a(t_e^1)] \\
& + 2r_{K^*} \phi_{K^*}^s(x_3, b_3) \alpha_s(t_e^2) h_e(x_3, x_1, b_3, b_1) \exp[-S_a(t_e^2)] \} , \quad (16)
\end{aligned}$$

where $C_F = 4/3$ is a color factor. The functions h_e^i , the scales t_e^i and the Sudakov factors $S_a(t_e^1)$ and $S_a(t_e^2)$ will be given explicitly in the Appendix. In Eq. (16), we do not include the Wilson coefficients of the corresponding operators, which are process dependent. They will be shown later in this section for different decay channels.

The form factor of B to K^* transition, $A_0^{B \rightarrow K^*}(0)$, can also be extracted from F_{eK^*} in Eq. (16), that is

$$A_0^{B \rightarrow K^*}(q^2 = 0) = \frac{\sqrt{2} F_{eK^*}}{G_F f_K m_B^2}. \quad (17)$$

The operators O_{5-8} have a structure of $(V - A)(V + A)$. Some of these operators contribute to the decay amplitude in a factorizable way. Since only the axial-vector part of $(V + A)$ current contribute to the pseudo-scalar meson production,

$$\langle K^* | V - A | B \rangle \langle K | V + A | 0 \rangle = -\langle K^* | V - A | B \rangle \langle K | V - A | 0 \rangle. \quad (18)$$

The contribution of these operators is opposite in sign with F_{eK^*} in Eq. (16):

$$F_{eK^*}^{P1} = -F_{eK^*}. \quad (19)$$

In some other cases, one needs to do Fierz transformation for these operators first and then get right color structure for factorization to work. In this case, one gets $(S - P)(S + P)$ operators from $(V - A)(V + A)$ ones. For these $(S - P)(S + P)$ operators, Figs. 2(a) and 2(b) gives

$$\begin{aligned} F_{eK^*}^{P2} = & 8\sqrt{2}G_F\pi C_F f_K r_K m_B^4 \int_0^1 dx_1 dx_3 \int_0^\infty b_1 db_1 b_3 db_3 \phi_B(x_1, b_1) \\ & \cdot \{ [\phi_{K^*}(x_3, b_3) + r_{K^*}((x_3 + 2)\phi_{K^*}^s(x_3, b_3) - x_3\phi_{K^*}^t(x_3, b_3))] \\ & \cdot \alpha_s(t_e^1) h_e(x_1, x_3, b_1, b_3) \exp[-S_a(t_e^1)] \\ & + (x_1\phi_{K^*}(x_3, b_3) + 2r_{K^*}\phi_{K^*}^s(x_3, b_3)) \alpha_s(t_e^2) h_e(x_3, x_1, b_3, b_1) \exp[-S_a(t_e^2)] \} \quad (20) \end{aligned}$$

For the non-factorizable diagram 2(c) and 2(d), all three meson wave functions are involved. The integration of b_3 can be performed using δ function $\delta(b_3 - b_1)$, leaving only integration of b_1 and b_2 . M_{eK^*} denotes the contribution from the operators of type $(V - A)(V - A)$, and $M_{eK^*}^{P1}$ is the contribution from the operators of type $(V - A)(V + A)$:

$$\begin{aligned} M_{eK^*} = & \frac{16}{\sqrt{3}}G_F\pi C_F m_B^4 \int_0^1 dx_1 dx_2 dx_3 \int_0^\infty b_1 db_1 b_2 db_2 \phi_B(x_1, b_1) \phi_K^A(x_2, b_2) \\ & \cdot \{ - [-x_2\phi_{K^*}(x_3, b_1) + r_{K^*}x_3 (\phi_{K^*}^s(x_3, b_1) - \phi_{K^*}^t(x_3, b_1))] \\ & \cdot \alpha_s(t_f) h_f^1(x_1, x_2, x_3, b_1, b_2) \exp[-S_c(t_f^1)] \\ & + [(x_2 - x_3 - 1)\phi_{K^*}(x_3, b_1) + r_{K^*}x_3 (\phi_{K^*}^s(x_3, b_1) + \phi_{K^*}^t(x_3, b_1))] \\ & \cdot \alpha_s(t_f) h_f^2(x_1, x_2, x_3, b_1, b_2) \exp[-S_c(t_f^2)] \} , \quad (21) \end{aligned}$$

$$\begin{aligned}
M_{eK^*}^{P_1} = & \frac{16}{\sqrt{3}} G_F \pi C_F m_B^4 \int_0^1 dx_1 dx_2 dx_3 \int_0^\infty b_1 db_1 b_2 db_2 \phi_B(x_1, b_1) r_K \\
& \cdot \left\{ \left[(x_1 - x_2) (\phi_K^P(x_2, b_2) - \phi_K^T(x_2, b_2)) \phi_{K^*}(x_3, b_1) + r_{K^*} (x_1 (\phi_K^P(x_2, b_2) \right. \right. \\
& - \phi_K^T(x_2, b_2)) (\phi_{K^*}^s(x_3, b_1) - \phi_{K^*}^t(x_3, b_1)) - x_2 (\phi_K^P(x_2, b_2) - \phi_K^T(x_2, b_2)) \\
& \cdot (\phi_{K^*}^s(x_3, b_1) - \phi_{K^*}^t(x_3, b_1)) - x_3 (\phi_K^P(x_2, b_2) + \phi_K^T(x_2, b_2)) (\phi_{K^*}^s(x_3, b_1) \\
& + \phi_{K^*}^t(x_3, b_1)) \left. \right] \alpha_s(t_f) h_f^1(x_1, x_2, x_3, b_1, b_2) \exp[-S_c(t_f^1)] \\
& - \left[(x_1 + x_2 - 1) (\phi_K^P(x_2, b_2) - \phi_K^T(x_2, b_2)) \phi_{K^*}(x_3, b_1) \right. \\
& + r_{K^*} (x_1 (\phi_K^P(x_2, b_2) - \phi_K^T(x_2, b_2)) (\phi_{K^*}^s(x_3, b_1) - \phi_{K^*}^t(x_3, b_1)) \\
& - (1 - x_2) (\phi_K^P(x_2, b_2) - \phi_K^T(x_2, b_2)) (\phi_{K^*}^s(x_3, b_1) - \phi_{K^*}^t(x_3, b_1)) \\
& - x_3 (\phi_K^P(x_2, b_2) + \phi_K^T(x_2, b_2)) (\phi_{K^*}^s(x_3, b_1) + \phi_{K^*}^t(x_3, b_1)) \left. \right] \\
& \left. \alpha_s(t_f) h_f^2(x_1, x_2, x_3, b_1, b_2) \exp[-S_c(t_f^2)] \right\} . \tag{22}
\end{aligned}$$

For the non-factorizable annihilation diagram 2(e), we have three kinds of contributions: M_{aK^*} for $(V - A)(V - A)$ operators, $M_{aK^*}^{P_1}$ for $(V - A)(V + A)$ operators and $M_{aK^*}^{P_2}$ for $(S - P)(S + P)$ operators.

$$\begin{aligned}
M_{aK^*} = & \frac{16}{\sqrt{3}} G_F \pi C_F m_B^4 \int_0^1 dx_1 dx_2 dx_3 \int_0^\infty b_1 db_1 b_2 db_2 \phi_B(x_1, b_1) \\
& \cdot \left\{ - \left[x_2 \phi_{K^*}(x_3, b_2) \phi_K^A(x_2, b_2) + r_{K^*} r_K (\phi_K^P(x_2, b_2) ((x_2 + x_3 + 2.) \right. \right. \\
& \cdot \phi_{K^*}^s(x_3, b_2) + (x_2 - x_3) \phi_{K^*}^t(x_3, b_2)) + \phi_K^T(x_2, b_2) (-x_3 (\phi_{K^*}^s(x_3, b_2) \\
& - \phi_{K^*}^t(x_3, b_2)) - 2\phi_{K^*}^t(x_3, b_2) + x_2 (\phi_{K^*}^s(x_3, b_2) + \phi_{K^*}^t(x_3, b_2))) \left. \right] \\
& \cdot \alpha_s(t_f^3) h_f^3(x_1, x_2, x_3, b_1, b_2) \exp[-S_c(t_f^3)] \\
& + \left[x_3 \phi_{K^*}(x_3, b_2) \phi_K^A(x_2, b_2) - r_{K^*} r_K (-x_2 (\phi_K^P(x_2, b_2) - \phi_K^T(x_2, b_2)) \right. \\
& \cdot (\phi_{K^*}^s - \phi_{K^*}^t) - x_3 (\phi_K^P(x_2, b_2) + \phi_K^T(x_2, b_2)) (\phi_{K^*}^s(x_3, b_2) + \phi_{K^*}^t(x_3, b_2)) \left. \right] \\
& \cdot \alpha_s(t_f^4) h_f^4(x_1, x_2, x_3, b_1, b_2) \exp[-S_c(t_f^4)] \left. \right\} , \tag{23}
\end{aligned}$$

where $r_K = m_0^K / m_B$ with $m_0^K = m_K^2 / (m_s + m_d)$.

$$\begin{aligned}
M_{aK^*}^{P_1} = & \frac{16}{\sqrt{3}} G_F \pi C_F m_B^4 \int_0^1 dx_1 dx_2 dx_3 \int_0^\infty b_1 db_1 b_2 db_2 \phi_B(x_1, b_1) \\
& \cdot \left\{ \left[-r_{K^*} (x_3 - 2) (\phi_{K^*}^s(x_3, b_2) + \phi_{K^*}^t(x_3, b_2)) \right. \right. \\
& + r_K (x_2 - 2) \phi_{K^*}(x_3, b_2) (\phi_K^P(x_2, b_2) + \phi_K^T(x_2, b_2)) \left. \right] \\
& \cdot \alpha_s(t_f^3) h_f^3(x_1, x_2, x_3, b_1, b_2) \exp[-S_c(t_f^3)] \\
& + \left[-x_2 r_K \phi_{K^*}(x_3, b_2) (\phi_K^P(x_2, b_2) + \phi_K^T(x_2, b_2)) \right. \\
& + x_3 r_{K^*} \phi_K^A(x_2, b_2) (\phi_{K^*}^s(x_3, b_2) + \phi_{K^*}^t(x_3, b_2)) \left. \right] \\
& \cdot \alpha_s(t_f^4) h_f^4(x_1, x_2, x_3, b_1, b_2) \exp[-S_c(t_f^4)] \left. \right\} . \tag{24}
\end{aligned}$$

$$\begin{aligned}
M_{aK^*}^{P_2} = & \frac{16}{\sqrt{3}} G_F \pi C_F m_B^4 \int_0^1 dx_1 dx_2 dx_3 \int_0^\infty b_1 db_1 b_2 db_2 \phi_B(x_1, b_1) \\
& \cdot \left\{ [x_3 \phi_{K^*}(x_3, b_2) \phi_K^A(x_2, b_2) + r_{K^*} r_K ((x_2 + x_3 + 2) \phi_{K^*}^s(x_3, b_2) \right. \\
& - (x_2 - x_3) \phi_{K^*}^t(x_3, b_2)) \phi_K^P(x_2, b_2) + (x_3 (\phi_{K^*}^s(x_3, b_2) + \phi_{K^*}^t(x_3, b_2)) \\
& + x_2 (\phi_{K^*}^t(x_3, b_2) - \phi_{K^*}^s(x_3, b_2)) - 2 \phi_{K^*}^t(x_3, b_2) \phi_K^T(x_2, b_2)] \\
& \cdot \alpha_s(t_f^3) h_f^3(x_1, x_2, x_3, b_1, b_2) \exp[-S_c(t_f^3)] \\
& + [-x_2 \phi_{K^*}(x_3, b_2) \phi_K^A(x_2, b_2) + r_{K^*} r_K (-x_2 (\phi_K^P(x_2, b_2) + \phi_K^T(x_2, b_2)) \\
& \cdot (\phi_{K^*}^s(x_3, b_2) + \phi_{K^*}^t(x_3, b_2)) - x_3 (\phi_K^P(x_2, b_2) - \phi_K^T(x_2, b_2)) \\
& \cdot (\phi_{K^*}^s(x_3, b_2) - \phi_{K^*}^t(x_3, b_2))] \alpha_s(t_f^4) h_f^4(x_1, x_2, x_3, b_1, b_2) \exp[-S_c(t_f^4)] \left. \right\} . \quad (25)
\end{aligned}$$

The factorizable annihilation diagram 2(g) involves only K^* and K wave functions. The decay amplitude F_{aK^*} , $F_{aK^*}^{P_1}$ and $F_{aK^*}^{P_2}$ represent the contributions from $(V - A)(V - A)$ operators, $(V - A)(V + A)$ operators and $(S - P)(S + P)$ operators, respectively.

$$\begin{aligned}
F_{aK^*} = & -4\sqrt{2}\pi G_F C_F f_B m_B^4 \int_0^1 dx_2 dx_3 \int_0^\infty b_2 db_2 b_3 db_3 \\
& \cdot \left\{ [x_3 \phi_{K^*}(x_3, b_3) \phi_K^A(x_2, b_2) + 2r_{K^*} r_K \phi_K^P(x_2, b_2) ((1 + x_3) \phi_{K^*}^s(x_3, b_3) \right. \\
& - (1 - x_3) \phi_{K^*}^t(x_3, b_3))] \alpha_s(t_e^3) h_a(x_2, x_3, b_2, b_3) \exp[-S_d(t_e^3)] \\
& - [x_2 \phi_{K^*}(x_3, b_3) \phi_K^A(x_2, b_2) + 2r_{K^*} r_K \phi_{K^*}^s(x_3, b_3) ((1 + x_2) \phi_K^P(x_2, b_2) \\
& - (1 - x_2) \phi_K^T(x_2, b_2))] \alpha_s(t_e^4) h_a(x_3, x_2, b_3, b_2) \exp[-S_d(t_e^4)] \left. \right\} , \quad (26)
\end{aligned}$$

$$F_{aK^*}^{P_1} = -F_{aK^*}, \quad (27)$$

$$\begin{aligned}
F_{aK^*}^{P_2} = & -8\sqrt{2}\pi G_F C_F m_B^4 f_B \int_0^1 dx_2 dx_3 \int_0^\infty b_2 db_2 b_3 db_3 \\
& \cdot \left\{ [2r_K \phi_{K^*}(x_3, b_3) \phi_K^P(x_2, b_2) + x_3 r_{K^*} (\phi_{K^*}^s(x_3, b_3) - \phi_{K^*}^t(x_3, b_3)) \phi_K^A(x_2, b_2)] \right. \\
& \cdot \alpha_s(t_e^3) h_a(x_2, x_3, b_2, b_3) \exp[-S_d(t_e^3)] \\
& + [2r_{K^*} \phi_{K^*}^s(x_3, b_3) \phi_K^A(x_2, b_2) + x_2 r_K (\phi_K^P(x_2, b_2) - \phi_K^T(x_2, b_2)) \phi_{K^*}(x_3, b_3)] \\
& \cdot \alpha_s(t_e^4) h_a(x_3, x_2, b_3, b_2) \exp[-S_d(t_e^4)] \left. \right\} . \quad (28)
\end{aligned}$$

In the above equations, we have assumed that $x_1 \ll x_2, x_3$. Since the light quark momentum fraction x_1 in B meson is peaked at the small x_1 region, while quark momentum fraction x_2 of K is peaked around 0.5, this is not a bad approximation. The numerical results also show that this approximation makes very little difference in the final result. After using this approximation, all the diagrams are functions of $k_1^- = x_1 m_B / \sqrt{2}$ of B meson only, independent of the variable of k_1^+ .

For the Feynman diagram 2(f) and 2(h), the corresponding decay amplitude is the same in structure as those for 2(e) and 2(g). We get the decay amplitude easily by making two replacements of $x_2 \rightarrow 1 - x_2$ and $x_3 \rightarrow 1 - x_3$ in the relevant distribution amplitudes.

For the case of $M_1 = K^0$ and $M_2 = \overline{K}^{*0}$, by following the same procedure, one can find all decay amplitudes: F_{eK} , $F_{eK}^{P_1}$ and $F_{eK}^{P_2}$, M_{eK} , $M_{eK}^{P_1}$, M_{aK} , $M_{aK}^{P_1}$ and $M_{aK}^{P_2}$, F_{aK} , $F_{aK}^{P_1}$ and $F_{aK}^{P_2}$. The explicit expressions of these decay amplitudes will be given in Appendix A.

B. Total Decay amplitudes

Based the isospin symmetry and the analytical results obtained in last subsection, one can derive out all the decay amplitudes for $B^0 \rightarrow K^+K^{*-}(K^{*+}K^-)$ and $B^+ \rightarrow K^+\bar{K}^{*0}(K^{*+}\bar{K}^0)$ decays.

Combining all contributions, the total decay amplitude for all considered decay modes can be written as:

$$\begin{aligned}
\mathcal{M}(B^0 \rightarrow K^0\bar{K}^{*0}) = & -\xi_t \left\{ F_{eK} \left(\frac{C_3}{3} + C_4 - \frac{C_9}{6} - \frac{C_{10}}{2} \right) + M_{eK} \left(C_3 - \frac{C_9}{2} \right) + M_{eK}^{P_1} \left(C_5 - \frac{C_7}{2} \right) \right. \\
& + M_{aK} \left(C_3 + C_4 - \frac{C_9}{2} - \frac{C_{10}}{2} \right) + M_{aK}^{P_1} \left(C_5 - \frac{C_7}{2} \right) + M_{aK}^{P_2} \left(C_6 - \frac{C_8}{2} \right) + M_{aK^*} \left(C_4 - \frac{C_{10}}{2} \right) \\
& + F_{aK} \left(\frac{4}{3}C_3 + \frac{4}{3}C_4 - C_5 - \frac{C_6}{3} + \frac{C_7}{2} + \frac{C_8}{6} - \frac{2}{3}C_9 - \frac{2}{3}C_{10} \right) + M_{aK^*}^{P_2} \left(C_6 - \frac{C_8}{2} \right) \\
& \left. + F_{aK^*} \left(C_3 + \frac{C_4}{3} - C_5 - \frac{C_6}{3} + \frac{C_7}{2} + \frac{C_8}{6} - \frac{C_9}{2} - \frac{C_{10}}{6} \right) + F_{aK^*}^{P_2} \left(\frac{C_5}{3} + C_6 - \frac{C_7}{6} - \frac{C_8}{2} \right) \right\} \quad (29)
\end{aligned}$$

$$\begin{aligned}
\mathcal{M}(B^0 \rightarrow K^{*0}\bar{K}^0) = & -\xi_t \left\{ F_{eK^*} \left(\frac{C_3}{3} + C_4 - \frac{C_9}{6} - \frac{C_{10}}{2} \right) + F_{eK^*}^{P_2} \left(\frac{C_5}{3} + C_6 - \frac{C_7}{6} - \frac{C_8}{2} \right) \right. \\
& + M_{eK^*} \left(C_3 - \frac{C_9}{2} \right) + M_{eK^*}^{P_1} \left(C_5 - \frac{C_7}{2} \right) + M_{aK^*} \left(C_3 + C_4 - \frac{C_9}{2} - \frac{C_{10}}{2} \right) \\
& + M_{aK^*}^{P_1} \left(C_5 - \frac{C_7}{2} \right) + M_{aK^*}^{P_2} \left(C_6 - \frac{C_8}{2} \right) + F_{aK^*}^{P_2} \left(\frac{C_5}{3} + C_6 - \frac{C_7}{6} - \frac{C_8}{2} \right) \\
& + F_{aK} \left(C_3 + \frac{C_4}{3} - C_5 - \frac{C_6}{3} + \frac{C_7}{2} + \frac{C_8}{6} - \frac{C_9}{2} - \frac{C_{10}}{6} \right) + M_{aK} \left(C_4 - \frac{C_{10}}{2} \right) \\
& \left. + F_{aK^*} \left(\frac{4}{3}C_3 + \frac{4}{3}C_4 - C_5 - \frac{C_6}{3} + \frac{C_7}{2} + \frac{C_8}{6} - \frac{2}{3}C_9 - \frac{2}{3}C_{10} \right) + M_{aK^*}^{P_2} \left(C_6 - \frac{C_8}{2} \right) \right\} \quad (30)
\end{aligned}$$

$$\begin{aligned}
\mathcal{M}(B^0 \rightarrow K^+K^{*-}) = & \xi_u \left[M_{aK}C_2 + F_{aK} \left(C_1 + \frac{C_2}{3} \right) \right] - \xi_t \left\{ M_{aK} (C_4 + C_{10}) + M_{aK^*}^{P_2} \left(C_6 - \frac{C_8}{2} \right) \right. \\
& + F_{aK} \left(C_3 + \frac{C_4}{3} - C_5 - \frac{C_6}{3} - C_7 - \frac{C_8}{3} + C_9 + \frac{C_{10}}{3} \right) + M_{aK}^{P_2} (C_6 + C_8) \\
& \left. + F_{aK^*} \left(C_3 + \frac{C_4}{3} - C_5 - \frac{C_6}{3} + \frac{C_7}{2} + \frac{C_8}{6} - \frac{1}{2}C_9 - \frac{C_{10}}{6} \right) + M_{aK^*} \left(C_4 - \frac{C_{10}}{2} \right) \right\} \quad (31)
\end{aligned}$$

$$\begin{aligned}
\mathcal{M}(B^0 \rightarrow K^{*+}K^-) = & \xi_u \left[M_{aK^*}C_2 + F_{aK^*} \left(C_1 + \frac{C_2}{3} \right) \right] \\
& - \xi_t \left\{ F_{aK} \left(C_3 + \frac{C_4}{3} - C_5 - \frac{C_6}{3} + \frac{C_7}{2} + \frac{C_8}{6} - \frac{C_9}{2} - \frac{C_{10}}{6} \right) \right. \\
& + F_{aK^*} \left(C_3 + \frac{C_4}{3} - C_5 - \frac{C_6}{3} - C_7 - \frac{C_8}{3} + C_9 + \frac{C_{10}}{3} \right) + M_{aK^*} (C_4 + C_{10}) \\
& \left. + M_{aK} \left(C_4 - \frac{C_{10}}{2} \right) + M_{aK}^{P_2} \left(C_6 - \frac{C_8}{2} \right) + M_{aK^*}^{P_2} (C_6 + C_8) \right\} \quad (32)
\end{aligned}$$

$$\begin{aligned}
\mathcal{M}(B^+ \rightarrow K^+ \bar{K}^{*0}) &= \xi_u \left(M_{aK} C_1 + F_{aK} \left(\frac{C_1}{3} + C_2 \right) \right) - \xi_t \left\{ F_{eK} \left(\frac{C_3}{3} + C_4 - \frac{C_9}{6} - \frac{C_{10}}{2} \right) \right. \\
&\quad + F_{aK}^{P_2} \left(\frac{C_5}{3} + C_6 + \frac{C_7}{3} + C_8 \right) + M_{eK} \left(C_3 - \frac{C_9}{2} \right) + M_{eK}^{P_1} \left(C_5 - \frac{C_7}{2} \right) \\
&\quad \left. + M_{aK} (C_3 + C_9) + M_{aK}^{P_1} (C_5 + C_7) + F_{aK} \left(\frac{C_3}{3} + C_4 + \frac{C_9}{3} + C_{10} \right) \right\} \quad (33)
\end{aligned}$$

$$\begin{aligned}
\mathcal{M}(B^+ \rightarrow K^{*+} \bar{K}^0) &= \xi_u \left(M_{aK^*} C_1 + F_{aK^*} \left(\frac{C_1}{3} + C_2 \right) \right) - \xi_t \left\{ F_{eK^*} \left(\frac{C_3}{3} + C_4 - \frac{C_9}{6} - \frac{C_{10}}{2} \right) \right. \\
&\quad + F_{eK^*}^{P_2} \left(\frac{C_5}{3} + C_6 - \frac{C_7}{6} - \frac{C_8}{2} \right) + F_{aK^*}^{P_2} \left(\frac{C_5}{3} + C_6 + \frac{C_7}{3} + C_8 \right) + M_{eK^*} \left(C_3 - \frac{C_9}{2} \right) \\
&\quad \left. + M_{eK^*}^{P_1} \left(C_5 - \frac{C_7}{2} \right) + M_{aK^*} (C_3 + C_9) + M_{aK^*}^{P_1} (C_5 + C_7) + F_{aK^*} \left(\frac{C_3}{3} + C_4 + \frac{C_9}{3} + C_{10} \right) \right\} \quad (34)
\end{aligned}$$

where $\xi_u = V_{ub}^* V_{ud}$, $\xi_t = V_{tb}^* V_{td}$. The exact expressions of individual transition amplitudes not given explicitly in this section, such as F_{aK} and M_{aK} , etc., are collected in the Appendix A.

The decay amplitudes for those charge-conjugated decay channels can be obtained from the results as given in Eqs.(29) - (34) by simple replacements of $\xi_u \rightarrow \xi_u^*$ and $\xi_t \rightarrow \xi_t^*$.

Analogous to Eq. (17), the form factor $F_{0,1}^{B \rightarrow K}(q^2 = 0)$ can also be extracted from F_{eK} via the following relation

$$F_{0,1}^{B \rightarrow K}(q^2 = 0) = \frac{\sqrt{2} F_{eK}}{G_F f_{K^*} m_B^2}. \quad (35)$$

IV. NUMERICAL RESULTS AND DISCUSSIONS

A. Input parameters and wave functions

Before we calculate the branching ratios and CP violating asymmetries for the B decays under study, we firstly present the input parameters to be used in the numerical calculations.

$$\begin{aligned}
\Lambda_{\overline{\text{MS}}}^{(f=4)} &= 0.25\text{GeV}, \quad f_B = 0.19\text{GeV}, \quad m_0^K = 1.7\text{GeV}, \\
f_{K^*} &= 0.217\text{GeV}, \quad f_{K^*}^T = f_K = 0.16\text{GeV}, \quad m_K = 0.497\text{GeV}, \\
m_{K^*} &= 0.89\text{GeV}, \quad M_B = 5.2792\text{GeV}, \quad M_W = 80.41\text{GeV}. \quad (36)
\end{aligned}$$

The central values of the CKM matrix elements to be used in numerical calculations are

$$\begin{aligned}
|V_{ud}| &= 0.9745, \quad |V_{ub}| = 0.0036, \\
|V_{tb}| &= 0.9990, \quad |V_{td}| = 0.0075. \quad (37)
\end{aligned}$$

For the B meson wave function, we adopt the model[15, 22, 24]

$$\phi_B(x, b) = N_B x^2 (1-x)^2 \exp \left[-\frac{M_B^2 x^2}{2\omega_b^2} - \frac{1}{2}(\omega_b b)^2 \right], \quad (38)$$

where the shape parameter $\omega_b = 0.4 \pm 0.04$ GeV has been constrained in other decay modes. The normalization constant $N_B = 91.745$ is related to $f_B = 0.19$ GeV and $\omega_b = 0.4$.

The K^* meson distribution amplitude up to twist-3 are given by [27] with QCD sum rules.

$$\phi_{K^*}(x) = \frac{3}{\sqrt{6}} f_{K^*} x(1-x) \left[1 + 0.57(1-2x) + 0.07 C_2^{3/2}(1-2x) \right], \quad (39)$$

$$\begin{aligned} \phi_{K^*}^t(x) = \frac{f_{K^*}^T}{2\sqrt{6}} \{ & 0.3(1-2x) (3(1-2x)^2 + 10(1-2x) - 1) \\ & + 1.68 C_4^{1/2}(1-2x) + 0.06(1-2x)^2 (5(1-2x)^2 - 3) \\ & + 0.36 [1 - 2(1-2x) - 2(1-2x) \ln(1-x)] \}, \end{aligned} \quad (40)$$

$$\begin{aligned} \phi_{K^*}^s(x) = \frac{f_{K^*}^T}{2\sqrt{6}} \{ & 3(1-2x) [1 + 0.2(1-2x) + 0.6(10x^2 - 10x + 1)] \\ & - 0.12x(1-x) + 0.36 [1 - 6x - 2 \ln(1-x)] \}, \end{aligned} \quad (41)$$

where the Gegenbauer polynomials are defined by

$$C_2^{3/2}(t) = \frac{3}{2} (5t^2 - 1), \quad C_4^{1/2}(t) = \frac{1}{8} (35t^4 - 30t^2 + 3). \quad (42)$$

For K meson, we use ϕ_K^A of twist-2 wave function and ϕ_K^P and ϕ_K^T of the twist-3 wavefunctions from [26, 27]

$$\phi_K^A(x) = \frac{3}{\sqrt{6}} f_K x(1-x) [1 + 0.51(1-2x) + 0.3 (5(1-2x)^2 - 1)], \quad (43)$$

$$\begin{aligned} \phi_K^P(x) = \frac{f_K}{2\sqrt{6}} [& 1 + 0.12(3(1-2x)^2 - 1) \\ & - 0.12 (3 - 30(1-2x)^2 + 35(1-2x)^4) / 8], \end{aligned} \quad (44)$$

$$\phi_K^T(x) = \frac{f_K}{2\sqrt{6}} (1-2x) [1 + 0.35 (10x^2 - 10x + 1)]. \quad (45)$$

Based on the definition of the form factor $A_0^{B \rightarrow K^*}$ and $F_{0,1}^{B \rightarrow K}$ as given in Eqs. (17) and (35), we find the numerical values of the corresponding form factors at zero momentum transfer.

$$\begin{aligned} A_0^{B \rightarrow K^*}(q^2 = 0) &= 0.46_{-0.06}^{+0.07}(\omega_b), \\ F_{0,1}^{B \rightarrow K}(q^2 = 0) &= 0.35_{-0.04}^{+0.06}(\omega_b). \end{aligned} \quad (46)$$

where the errors are induced by the change of ω_b for $\omega_b = 0.40 \pm 0.04$ GeV. These results are close to the light-cone QCD sum rule predictions [28]

$$\begin{aligned} A_0^{B \rightarrow K^*}(q^2 = 0) &= 0.374 \pm 0.034, \\ F_{0,1}^{B \rightarrow K}(q^2 = 0) &= 0.331 \pm 0.041 \end{aligned} \quad (47)$$

B. Branching ratios

In order to calculate the branching ratios and CP asymmetries in a more clear way, we rewrite the decay amplitudes as given in Eqs.(29)-(34) in a new form

$$\mathcal{M} = V_{ub}^* V_{ud} T - V_{tb}^* V_{td} P = V_{ub}^* V_{ud} T [1 + z e^{i(\alpha+\delta)}], \quad (48)$$

where the term ‘‘T’’ and ‘‘P’’ denote the ‘‘Tree’’ and ‘‘Penguin’’ part of a given decay amplitude \mathcal{M} , which is proportional to $\xi_u = V_{ub}^* V_{ud}$ or $\xi_t = V_{tb}^* V_{td}$, respectively. While the ratio

$$z = \left| \frac{V_{tb}^* V_{td}}{V_{ub}^* V_{ud}} \right| \left| \frac{P}{T} \right| \quad (49)$$

is proportional to the ratio of penguin (P) to tree (T) contributions, the CKM angle $\alpha = \arg \left[-\frac{V_{td} V_{tb}^*}{V_{ud} V_{ub}^*} \right]$ is the weak phase, and δ is the relative strong phase between the tree and penguin part.

Take $\mathcal{M}(B^+ \rightarrow K^+ \bar{K}^{*0})$ in Eq. (33) as an example, its ‘‘T’’ and ‘‘P’’ parts can be written as in the form of

$$\begin{aligned} T &= M_{aK} C_1 + F_{aK} \left(\frac{1}{3} C_1 + C_2 \right), \\ P &= F_{eK} \left(\frac{1}{3} C_3 + C_4 - \frac{1}{6} C_9 - \frac{1}{2} C_{10} \right) + F_{aK}^{P_2} \left(\frac{1}{3} C_5 + C_6 + \frac{1}{3} C_7 + C_8 \right) \\ &\quad + M_{eK} \left(C_3 - \frac{1}{2} C_9 \right) + M_{eK}^{P_1} \left(C_5 - \frac{1}{2} C_7 \right) + M_{aK} (C_3 + C_9) \\ &\quad + M_{aK}^{P_1} (C_5 + C_7) + F_{aK} \left(\frac{1}{3} C_3 + C_4 + \frac{1}{3} C_9 + C_{10} \right). \end{aligned} \quad (50)$$

$$(51)$$

In pQCD approach, the ratio z and the strong phase δ can be calculated perturbatively. For $B^+ \rightarrow K^+ \bar{K}^{*0}$ and $K^{*+} \bar{K}^0$ decays, for example, we find numerically that

$$\begin{aligned} z(K^+ \bar{K}^{*0}) &= 2.1, & \delta(K^+ \bar{K}^{*0}) &= -13^\circ, \\ z(K^{*+} \bar{K}^0) &= 2.7, & \delta(K^{*+} \bar{K}^0) &= -44^\circ. \end{aligned} \quad (52)$$

The major error of the ratio z and the strong phase δ is induced by the uncertainty of $\omega_b = 0.4 \pm 0.04$ GeV but is small in magnitude. The reason is that the errors induced by the uncertainties of input parameters are largely canceled in the ratio.

From Eq. (48), it is easy to write the decay amplitude for the corresponding charge conjugated decay mode

$$\overline{\mathcal{M}} = V_{ub} V_{ud}^* T - V_{tb} V_{td}^* P = V_{ub} V_{ud}^* T [1 + z e^{i(-\alpha+\delta)}]. \quad (53)$$

Therefore the CP-averaged branching ratio for $B^0 \rightarrow K K^*$ decay can be defined as

$$Br = (|\mathcal{M}|^2 + |\overline{\mathcal{M}}|^2)/2 = |V_{ub} V_{ud}^* T|^2 [1 + 2z \cos \alpha \cos \delta + z^2], \quad (54)$$

where the ratio z and the strong phase δ have been defined in Eqs. (48) and (49).

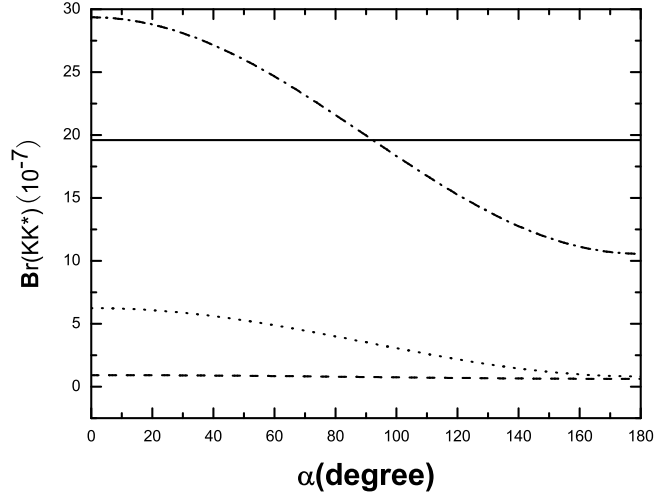


FIG. 5: Branching ratios (in units of 10^{-7}) of $B^+ \rightarrow K^{*+}\bar{K}^0$ (dash-dotted curve), $B^+ \rightarrow K^+\bar{K}^{*0}$ (dotted curve), $B^0/\bar{B}^0 \rightarrow K^0\bar{K}^{*0} + \bar{K}^0 K^{*0}$ (solid curve), $B^0/\bar{B}^0 \rightarrow K^+K^{*-} + K^-K^{*+}$ (dashed curve) as a function of CKM angle α .

It is a little complicate for us to calculate the branch ratios of $B^0/\bar{B}^0 \rightarrow f(\bar{f})$, since both B^0 and \bar{B}^0 can decay into the final state f and \bar{f} simultaneously. Due to $B^0 - \bar{B}^0$ mixing, it is very difficult to distinguish B^0 from \bar{B}^0 . But it is easy to identify the final states. Therefore we sum up $B^0/\bar{B}^0 \rightarrow K^0\bar{K}^{*0}$ as one channel, and $B^0/\bar{B}^0 \rightarrow \bar{K}^0 K^{*0}$ as another, although the summed up channels are not charge conjugate states [29]. Similarly, we have $B^0/\bar{B}^0 \rightarrow K^+K^{*-}$ as one channel, and $B^0/\bar{B}^0 \rightarrow K^-K^{*+}$ as another. We show the branching ratio of $B^0/\bar{B}^0 \rightarrow K^+K^{*-}$, $B^0/\bar{B}^0 \rightarrow K^-K^{*+}$, $B^+ \rightarrow K^+\bar{K}^{*0}$ and $B^+ \rightarrow K^{*+}\bar{K}^0$ decays as a function of α in Fig. 5.

Using the wave functions and the input parameters as specified previously, it is straightforward to calculate the branching ratios for the four considered decays. The pQCD predictions for the branching ratios are the following

$$Br(B^+ \rightarrow K^+\bar{K}^{*0}) = 3.1_{-0.8}^{+1.2}(\omega_b) \times 10^{-7}, \quad (55)$$

$$Br(B^+ \rightarrow K^{*+}\bar{K}^0) = 18.3_{-4.7}^{+6.8}(\omega_b) \times 10^{-7}, \quad (56)$$

$$Br(B^0/\bar{B}^0 \rightarrow K^0\bar{K}^{*0} + \bar{K}^0 K^{*0}) = 19.6_{-5.4}^{+7.9}(\omega_b) \times 10^{-7}, \quad (57)$$

$$Br(B^0/\bar{B}^0 \rightarrow K^+K^{*-} + K^-K^{*+}) = 7.4_{-1.3}^{+1.0}(\omega_b) \times 10^{-8}, \quad (58)$$

where the major error is induced by the uncertainty of $\omega_b = 0.4 \pm 0.04$ GeV.

As a comparison, we also list the theoretical predictions in QCDF approach [4]:

$$Br(B^- \rightarrow K^- K^{*0}) = 3.0_{-2.5}^{+6.0} \times 10^{-7}, \quad (59)$$

$$Br(B^- \rightarrow K^{*-} K^0) = 3.0_{-2.7}^{+7.2} \times 10^{-7}, \quad (60)$$

$$Br(\bar{B}^0 \rightarrow \bar{K}^0 K^{*0}) = 2.6_{-2.0}^{+4.8} \times 10^{-7}, \quad (61)$$

$$Br(\bar{B}^0 \rightarrow K^0 \bar{K}^{*0}) = 2.9_{-2.7}^{+7.3} \times 10^{-7}, \quad (62)$$

$$Br(\bar{B}^0 \rightarrow K^- K^{*+}) = 1.4_{-1.4}^{+10.7} \times 10^{-8}, \quad (63)$$

$$Br(\bar{B}^0 \rightarrow K^+ K^{*-}) = 1.4_{-1.4}^{+10.7} \times 10^{-8}, \quad (64)$$

where the individual errors as given in Refs. [4] have been added in quadrature. For $B^- \rightarrow K^- K^{*0}$ decay, the pQCD and QCDF predictions agree very well. For remaining decay modes, the pQCD predictions are larger than the QCDF predictions by a factor of 2 to 5, although they are still consistent with each other within errors because the theoretical uncertainties are still very large. When compared with the experimental upper limits, the theoretical predictions in both approaches still agree with the data. The large differences between the pQCD and QCDF predictions will be tested by the forthcoming precision measurements.

C. CP-violating asymmetries

Now we turn to the evaluations of the CP-violating asymmetries of $B \rightarrow KK^*$ decays in the pQCD approach. For $B^+ \rightarrow K^+ \bar{K}^{*0}$ and $B^+ \rightarrow K^{*+} \bar{K}^0$ decays, the direct CP-violating asymmetries A_{CP}^{dir} can be defined as:

$$A_{CP}^{dir} = \frac{|\overline{\mathcal{M}}|^2 - |\mathcal{M}|^2}{|\overline{\mathcal{M}}|^2 + |\mathcal{M}|^2} = \frac{2z \sin \alpha \sin \delta}{1 + 2z \cos \alpha \cos \delta + z^2}, \quad (65)$$

where the ratio z and the strong phase δ have been defined in previous subsection and are calculable in PQCD approach.

Using the definition in Eq.(65), it is easy to calculate the direct CP-violating asymmetries for $B^\pm \rightarrow K^\pm \bar{K}^{*0}(K^{*0})$ and $B^\pm \rightarrow K^{*\pm} \bar{K}^0(K^0)$ decays. The numerical results are

$$\begin{aligned} A_{CP}^{dir}(B^\pm \rightarrow K^\pm \bar{K}^{*0}(K^{*0})) &= -0.20 \pm 0.05(\alpha) \pm 0.02(\omega_b), \\ A_{CP}^{dir}(B^\pm \rightarrow K^{*\pm} \bar{K}^0(K^0)) &= -0.49_{-0.03}^{+0.07}(\alpha) \pm 0.07(\omega_b). \end{aligned} \quad (66)$$

for $\alpha = 100^\circ \pm 20^\circ$ and $\omega_b = 0.40 \pm 0.04$ GeV. These pQCD predictions are also consistent with those in QCDF approach [4]:

$$\begin{aligned} A_{CP}^{dir}(B^\pm \rightarrow K^\pm \bar{K}^{*0}(K^{*0})) &= -0.24_{-0.39}^{+0.28}, \\ A_{CP}^{dir}(B^\pm \rightarrow K^{*\pm} \bar{K}^0(K^0)) &= -0.13_{-0.37}^{+0.29}. \end{aligned} \quad (67)$$

where the individual errors as given in Ref. [4] have been added in quadrature. In Fig. 6, we show the α -dependence of the pQCD predictions of A_{CP}^{dir} for $B^\pm \rightarrow K^\pm \bar{K}^{*0}(K^{*0})$ (the solid curve) and $B^\pm \rightarrow K^{*\pm} \bar{K}^0(K^0)$ decay (the dotted curve), respectively.

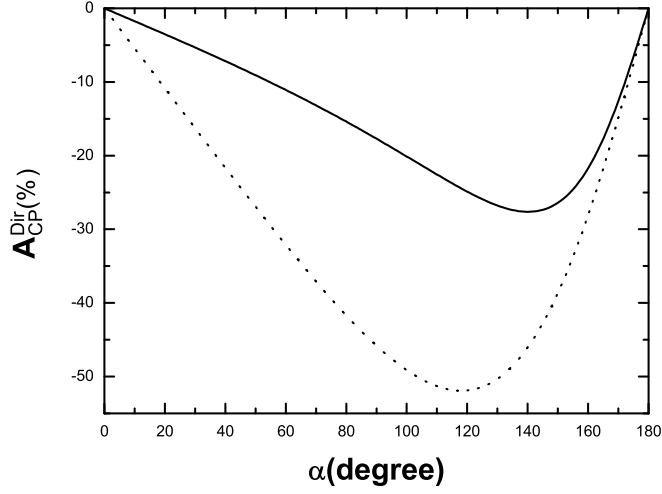


FIG. 6: The direct CP asymmetry A_{CP}^{dir} (in percentage) of $B^+ \rightarrow K^+ \bar{K}^{*0}$ (the solid curve) and $B^+ \rightarrow K^{*+} \bar{K}^0$ (the dotted curve) as a function of CKM angle α .

For $B^0/\bar{B}^0 \rightarrow K^0 \bar{K}^{*0} (\bar{K}^0 K^{*0})$ decays, they do not exhibit CP violating asymmetry, since they involve only penguin contributions at the leading order, as can be seen from the decay amplitudes as given in Eqs. (29) and (30).

We now study the CP-violating asymmetries for $B^0/\bar{B}^0 \rightarrow K^+ K^{*-} (K^- K^{*+})$ decays. Since both B^0 and \bar{B}^0 can decay to the final state $K^+ K^{*-}$ and $K^{*+} K^-$, there are four decay modes. Here we use the formulae as given in Ref. [29]. The four time-dependent decay widths for $B^0(t) \rightarrow K^+ K^{*-}, \bar{B}^0(t) \rightarrow K^- K^{*+}, B^0(t) \rightarrow K^- K^{*+}$ and $\bar{B}^0(t) \rightarrow K^+ K^{*-}$ can be expressed by four basic matrix elements[29]:

$$\begin{aligned} g &= \langle K^+ K^{*-} | H_{eff} | B^0 \rangle, & h &= \langle K^+ K^{*-} | H_{eff} | \bar{B}^0 \rangle, \\ \bar{g} &= \langle K^- K^{*+} | H_{eff} | \bar{B}^0 \rangle, & \bar{h} &= \langle K^- K^{*+} | H_{eff} | B^0 \rangle, \end{aligned} \quad (68)$$

which determines the decay matrix elements of $B^0 \rightarrow K^+ K^{*-}, \bar{B}^0 \rightarrow K^- K^{*+}, B^0 \rightarrow K^- K^{*+}$ and $\bar{B}^0 \rightarrow K^+ K^{*-}$ at $t=0$. The matrix elements g and \bar{h} are given in Eqs.(31) and (32). The matrix elements h and \bar{g} are obtained from \bar{h} and g by simple replacements of $\xi_u \rightarrow \xi_u^*$ and $\xi_t \rightarrow \xi_t^*$: i.e., changing the sign of the weak phases contained in the products of the CKM matrix elements ξ_u and ξ_t .

Following the general procedure, the $B^0 - \bar{B}^0$ mixing can be defined as

$$B_1 = p|B^0\rangle + q|\bar{B}^0\rangle, \quad B_2 = p|B^0\rangle - q|\bar{B}^0\rangle, \quad (69)$$

with $|p|^2 + |q|^2 = 1$. Following the notation of Ref. [29], the four time-dependent decay

widths of the considered decay modes can be written as

$$\begin{aligned}
\Gamma(B^0(t) \rightarrow K^+ K^{*-}) &= e^{-\Gamma t} \frac{1}{2} (|g|^2 + |h|^2) \times \{1 + a_{\epsilon'} \cos(\Delta mt) + a_{\epsilon+\epsilon'} \sin(\Delta mt)\}, \\
\Gamma(\overline{B}^0(t) \rightarrow K^+ K^{*-}) &= e^{-\Gamma t} \frac{1}{2} (|g|^2 + |h|^2) \times \{1 - a_{\epsilon'} \cos(\Delta mt) - a_{\epsilon+\epsilon'} \sin(\Delta mt)\}, \\
\Gamma(\overline{B}^0(t) \rightarrow K^- K^{*+}) &= e^{-\Gamma t} \frac{1}{2} (|\overline{g}|^2 + |\overline{h}|^2) \times \{1 - a_{\overline{\epsilon}'} \cos(\Delta mt) - a_{\epsilon+\overline{\epsilon}'} \sin(\Delta mt)\}, \\
\Gamma(B^0(t) \rightarrow K^- K^{*+}) &= e^{-\Gamma t} \frac{1}{2} (|\overline{g}|^2 + |\overline{h}|^2) \times \{1 + a_{\overline{\epsilon}'} \cos(\Delta mt) + a_{\epsilon+\overline{\epsilon}'} \sin(\Delta mt)\}, \quad (70)
\end{aligned}$$

where the four CP violating parameters are defined as

$$\begin{aligned}
a_{\epsilon'} &= \frac{|g|^2 - |h|^2}{|g|^2 + |h|^2}, & a_{\epsilon+\epsilon'} &= \frac{-2Im(\frac{g}{p} \frac{h}{g})}{1 + |h/g|^2} \\
a_{\overline{\epsilon}'} &= \frac{|\overline{h}|^2 - |\overline{g}|^2}{|\overline{h}|^2 + |\overline{g}|^2}, & a_{\epsilon+\overline{\epsilon}'} &= \frac{-2Im(\frac{g}{p} \frac{\overline{g}}{h})}{1 + |\overline{g}/\overline{h}|^2}, \quad (71)
\end{aligned}$$

where $q/p = e^{2i\beta}$. Using the decay amplitudes as given in Eqs. (31) and (32), it is straightforward to calculate the above four CP-violation parameters. The central values of the pQCD predictions are

$$\begin{aligned}
a_{\epsilon'} &= 0.74, & a_{\epsilon+\epsilon'} &= 0.68, \\
a_{\overline{\epsilon}'} &= 0.25, & a_{\epsilon+\overline{\epsilon}'} &= -0.88, \quad (72)
\end{aligned}$$

for $\alpha = 100^\circ$. The α -dependence of these four CP violating parameters are shown in Fig. 7. It is difficult to measure these physical observables in current and forthcoming B meson experiments because of its tiny branching ratio ($\sim 10^{-8}$).

At last, we will say a little more about the possible FSI effects. As mentioned in the introduction, we here do not consider the possible FSI effects on the branching ratios and CP-violating asymmetries of the $B \rightarrow KK^*$ decays. The FSI effect is in nature a subtle and complicated subject. The smallness of FSI effects has been put forward by Bjorken [30] based on the color transparency argument [5], and also supported by further renormalization group analysis of soft gluon exchanges among initial and final state mesons [20]. At present, the excellent agreement between the pQCD predictions for the branching ratios and CP violating asymmetries and the precision measurements strongly support the assumption that the FSI effects for $B \rightarrow K\pi$ decays are not important [7]. For $B \rightarrow KK$ decays, fortunately, good agreement between the pQCD predictions for the branching ratios of $B^+ \rightarrow K^+ K^0$, $B^0 \rightarrow K^+ K^-$ and $K^0 \overline{K}^0$ decays [15, 16] and currently available experimental measurements [19] indicates that the FSI effects are most possibly not important also [16]. Of course, more studies are needed about this issue, while further consistency check between the pQCD predictions and the precision data will reveal whether FSI effects are important or not.

V. SUMMARY

In this paper, we calculate the branching ratios and CP-violating asymmetries of $B^0/\overline{B}^0 \rightarrow K^0 \overline{K}^{*0}$ ($\overline{K}^0 K^{*0}$), $B^0/\overline{B}^0 \rightarrow K^+ K^{*-}$ ($K^- K^{*+}$), $B^+ \rightarrow K^+ \overline{K}^{*0}$, and $B^+ \rightarrow$

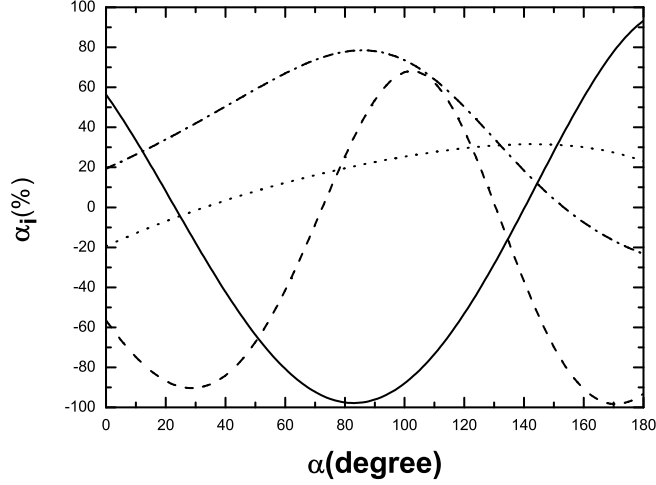


FIG. 7: CP violating parameters of $B^0/\bar{B}^0 \rightarrow K^+K^{*-}(K^-K^{*+})$ decays: a_{ϵ} (dash-dotted line), $a_{\epsilon'}$ (dotted line), $a_{\epsilon+\epsilon'}$ (dashed line) and $a_{\epsilon+\epsilon'}$ (solid line) as a function of CKM angle α

$K^{*+}\bar{K}^0$ decays, together with their charge-conjugated modes, by employing the pQCD factorization approach.

From our calculations and phenomenological analysis, we found the following results:

- The pQCD predictions for the form factors of $B \rightarrow K$ and K^* transitions are

$$F_{0,1}^{B \rightarrow K}(0) = 0.35_{-0.04}^{+0.06}, \quad A_0^{B \rightarrow K^*} = 0.46_{-0.06}^{+0.07}, \quad (73)$$

for $\omega_b = 0.40 \pm 0.04$ GeV, close to the light-cone QCD sum rule results [28].

- the pQCD predictions for the CP-averaged branching ratios are

$$\begin{aligned} Br(B^+ \rightarrow K^+\bar{K}^{*0}) &\approx 3.1 \times 10^{-7}, \\ Br(B^+ \rightarrow K^{*+}\bar{K}^0) &\approx 18.3 \times 10^{-7}, \\ Br(B^0/\bar{B}^0 \rightarrow K^0\bar{K}^{*0} + \bar{K}^0 K^{*0}) &\approx 19.6 \times 10^{-7}, \\ Br(B^0/\bar{B}^0 \rightarrow K^+K^{*-} + K^-K^{*+}) &\approx 7.4 \times 10^{-8}. \end{aligned} \quad (74)$$

The above pQCD predictions agree with the QCDF predictions within still large theoretical errors and close to currently available experimental upper limits.

- For the CP-violating asymmetries of the considered decay modes, the pQCD predictions are generally large in magnitude.

Acknowledgments

We are very grateful to Xin Liu and Hui-sheng Wang for helpful discussions. This work is partly supported by the National Natural Science Foundation of China under

Grant No.10275035 and 10575052, by the Specialized Research Fund for the doctoral Program of higher education (SRFDP) under Grant No. 20050319008, and by the Research Foundation of Jiangsu Education Committee under Grant No.2003102TSJB137.

APPENDIX A: NON-ZERO TRANSITION AMPLITUDES

The factorizable amplitudes F_{eK^*} , $F_{eK^*}^{P1}$ and $F_{eK^*}^{P2}$, F_{aK^*} , $F_{aK^*}^{P1}$ and $F_{aK^*}^{P2}$ have been given in Sec. III. The remaining factorizable transition amplitudes in $B \rightarrow KK^*$ decays are written as:

$$F_{eK} = 4\sqrt{2}\pi G_F C_F f_{K^*} m_B^4 \int_0^1 dx_1 dx_3 \int_0^\infty b_1 db_1 b_3 db_3 \phi_B(x_1, b_1) \cdot \left\{ \left[(1+x_3)\phi_K^A(x_3, b_3) + r_K(1-2x_3) \left(\phi_K^P(x_3, b_3) + \phi_K^T(x_3, b_3) \right) \right] \cdot \alpha_s(t_e^1) h_e(x_1, x_3, b_1, b_3) \exp[-S_a(t_e^1)] + 2r_K \phi_K^P(x_3, b_3) \alpha_s(t_e^2) h_e(x_3, x_1, b_3, b_1) \exp[-S_a(t_e^2)] \right\}, \quad (\text{A1})$$

$$F_{eK}^{P1} = F_{eK}, \quad (\text{A2})$$

$$F_{aK} = 4\sqrt{2}\pi G_F C_F f_B m_B^4 \int_0^1 dx_2 dx_3 \int_0^\infty b_2 db_2 b_3 db_3 \cdot \left\{ \left[x_3 \phi_{K^*}(x_3, b_3) \phi_K^A(x_2, b_2) + 2r_{K^*} r_K \phi_K^P(x_2, b_2) \left((1+x_3)\phi_{K^*}^s(x_3, b_3) - (1-x_3)\phi_{K^*}^t(x_3, b_2) \right) \right] \alpha_s(t_e^3) h_a(x_2, x_3, b_2, b_3) \exp[-S_d(t_e^3)] - \left[x_2 \phi_{K^*}(x_3, b_3) \phi_K^A(x_2, b_2) + 2r_{K^*} r_K \phi_{K^*}^s(x_3, b_3) \left((1+x_2)\phi_K^P(x_2, b_2) - (1-x_2)\phi_K^T(x_2, b_2) \right) \right] \alpha_s(t_e^4) h_a(x_3, x_2, b_3, b_2) \exp[-S_d(t_e^4)] \right\}, \quad (\text{A3})$$

$$F_{aK}^{P1} = -F_{aK}, \quad (\text{A4})$$

$$F_{aK}^{P2} = 8\sqrt{2}G_F \pi C_F m_B^4 f_B \int_0^1 dx_2 dx_3 \int_0^\infty b_2 db_2 b_3 db_3 \cdot \left\{ \left[2r_K \phi_{K^*}(x_3, b_3) \phi_K^P(x_2, b_2) + x_3 r_{K^*} \left(\phi_{K^*}^s(x_3, b_3) - \phi_{K^*}^t(x_3, b_2) \right) \phi_K^A(x_2, b_2) \right] \cdot \alpha_s(t_e^3) h_a(x_2, x_3, b_2, b_3) \exp[-S_d(t_e^3)] + \left[2r_{K^*} \phi_{K^*}^s(x_3, b_3) \phi_K^A(x_2, b_2) + x_2 r_K \left(\phi_K^P(x_2, b_2) - \phi_K^T(x_2, b_2) \right) \phi_{K^*}(x_3, b_3) \right] \cdot \alpha_s(t_e^4) h_a(x_3, x_2, b_3, b_2) \exp[-S_d(t_e^4)] \right\}. \quad (\text{A5})$$

For $B \rightarrow KK^*$ decays, the non-factorizable transition amplitudes not shown explicitly in Sec. III are written as:

$$M_{eK} = -\frac{16}{\sqrt{3}}G_F \pi C_F m_B^4 \int_0^1 dx_1 dx_2 dx_3 \int_0^\infty b_1 db_1 b_2 db_2 \phi_B(x_1, b_1) \phi_{K^*}(x_2, b_2) \cdot \left\{ \left[-x_2 \phi_K^A(x_3, b_2) + r_K x_3 \left(\phi_K^P(x_3, b_2) - \phi_K^T(x_3, b_2) \right) \right] \cdot \alpha_s(t_f^1) h_f^1(x_1, x_2, x_3, b_1, b_2) \exp[-S_b(t_f^1)] - \left[(x_2 - x_3 - 1)\phi_K^A(x_3, b_2) + r_K x_3 \left(\phi_K^P(x_3, b_2) + \phi_K^T(x_3, b_2) \right) \right] \cdot \alpha_s(t_f^2) h_f^2(x_1, x_2, x_3, b_1, b_2) \exp[-S_b(t_f^2)] \right\}, \quad (\text{A6})$$

$$\begin{aligned}
M_{eK}^{P_1} = & -\frac{16}{\sqrt{3}}G_F\pi C_{Fr}r_{K^*}m_B^4 \int_0^1 dx_1 dx_2 dx_3 \int_0^\infty b_1 db_1 b_2 db_2 \phi_B(x_1, b_1) \\
& \cdot \left\{ [x_2 \phi_K^A(x_3, b_2) (\phi_{K^*}^s(x_2, b_2) - \phi_{K^*}^t(x_2, b_2)) - r_K (x_1 (\phi_K^P(x_3, b_2) \right. \\
& - \phi_K^T(x_3, b_2)) (\phi_{K^*}^s(x_2, b_2) - \phi_{K^*}^t(x_2, b_2)) - x_2 (\phi_K^P(x_3, b_2) \\
& - \phi_K^T(x_3, b_2)) (\phi_{K^*}^s(x_2, b_2) - \phi_{K^*}^t(x_2, b_2)) - x_3 (\phi_K^P(x_3, b_2) + \phi_K^T(x_3, b_2)) \\
& \cdot (\phi_{K^*}^s(x_2, b_2) + \phi_{K^*}^t(x_2, b_2))] \alpha_s(t_f^1) h_f^1(x_1, x_2, x_3, b_1, b_2) \exp[-S_b(t_f^1)] \\
& + [(1-x_2)\phi_K^A(x_3, b_2) (\phi_{K^*}^s(x_2, b_2) - \phi_{K^*}^t(x_2, b_2)) - r_K (x_1 (\phi_K^P(x_3, b_2) \\
& - \phi_K^T(x_3, b_2)) (\phi_{K^*}^s(x_2, b_2) - \phi_{K^*}^t(x_2, b_2)) - (1-x_2) (\phi_K^P(x_3, b_2) \\
& - \phi_K^T(x_3, b_2)) (\phi_{K^*}^s(x_2, b_2) - \phi_{K^*}^t(x_2, b_2)) - x_3 (\phi_K^P(x_3, b_2) + \phi_K^T(x_3, b_2)) \\
& \cdot (\phi_{K^*}^s(x_2, b_2) + \phi_{K^*}^t(x_2, b_2))] \alpha_s(t_f^2) h_f^2(x_1, x_2, x_3, b_1, b_2) \exp[-S_b(t_f^2)] \Big\}, \quad (A7)
\end{aligned}$$

$$\begin{aligned}
M_{aK} = & -\frac{16}{\sqrt{3}}\pi G_F C_{Fm} m_B^4 \int_0^1 dx_1 dx_2 dx_3 \int_0^\infty b_1 db_1 b_2 db_2 \phi_B(x_1, b_1) \\
& \cdot \left\{ [x_2 \phi_{K^*}(x_2, b_2) \phi_K^A(x_3, b_2) + r_{K^*} r_K (((x_2 + x_3 + 2) \phi_{K^*}^s(x_2, b_2) \right. \\
& + (x_2 - x_3) \phi_{K^*}^t(x_2, b_2)) \phi_K^P(x_3, b_2) + \phi_K^T(x_3, b_2) (-x_3 (\phi_{K^*}^s(x_2, b_2) \\
& - \phi_{K^*}^t(x_2, b_2)) - 2\phi_{K^*}^t(x_2, b_2) + x_2 (\phi_{K^*}^s(x_2, b_2) + \phi_{K^*}^t(x_2, b_2)))] \\
& \cdot \alpha_s(t_f^3) h_f^3(x_1, x_2, x_3, b_1, b_2) \exp[-S_c(t_f^3)] \\
& - [x_3 \phi_{K^*}(x_2, b_2) \phi_K^A(x_3, b_2) + r_{K^*} r_K (x_2 (\phi_K^P(x_3, b_2) - \phi_K^T(x_3, b_2)) \\
& \cdot (\phi_{K^*}^s(x_2, b_2) - \phi_{K^*}^t(x_2, b_2)) + x_3 (\phi_K^P(x_3, b_2) + \phi_K^T(x_3, b_2)) \\
& \cdot (\phi_{K^*}^s(x_2, b_2) + \phi_{K^*}^t(x_2, b_2))] \alpha_s(t_f^4) h_f^4(x_1, x_2, x_3, b_1, b_2) \exp[-S_c(t_f^4)] \Big\}, \quad (A8)
\end{aligned}$$

$$M_{aK}^{P_1} = M_{aK^*}^{P_1}, \quad (A9)$$

$$M_{aK}^{P_2} = M_{aK^*}^{P_2}, \quad (A10)$$

where $r_K = m_0^K/m_B$ with $m_0^K = m_K^2/(m_s + m_d)$.

APPENDIX B: RELATED FUNCTIONS

We show here the function h_i 's, coming from the Fourier transformations of $H^{(0)}$,

$$\begin{aligned}
h_e(x_1, x_3, b_1, b_3) = & K_0(\sqrt{x_1 x_3} m_B b_1) [\theta(b_1 - b_3) K_0(\sqrt{x_3} m_B b_1) I_0(\sqrt{x_3} m_B b_3) \\
& + \theta(b_3 - b_1) K_0(\sqrt{x_3} m_B b_3) I_0(\sqrt{x_3} m_B b_1)] S_t(x_3), \quad (B1)
\end{aligned}$$

$$\begin{aligned}
h_a(x_2, x_3, b_2, b_3) = & K_0(i\sqrt{x_2 x_3} m_B b_2) [\theta(b_3 - b_2) K_0(i\sqrt{x_3} m_B b_3) I_0(i\sqrt{x_3} m_B b_2) \\
& + \theta(b_2 - b_3) K_0(i\sqrt{x_3} m_B b_2) I_0(i\sqrt{x_3} m_B b_3)] S_t(x_3), \quad (B2)
\end{aligned}$$

$$\begin{aligned}
h_f^{(j)}(x_1, x_2, x_3, b_1, b_2) = & \left\{ \theta(b_2 - b_1) I_0(M_B \sqrt{x_1 x_3} b_1) K_0(M_B \sqrt{x_1 x_3} b_2) \right. \\
& \left. + (b_1 \leftrightarrow b_2) \right\} \cdot \left(\begin{array}{ll} K_0(M_B D_{(j)} b_2), & \text{for } D_{(j)}^2 > 0 \\ \frac{\pi i}{2} H_0^{(1)}(M_B \sqrt{|D_{(j)}^2|} b_2), & \text{for } D_{(j)}^2 < 0 \end{array} \right), \quad (B3)
\end{aligned}$$

$$h_f^3(x_1, x_2, x_3, b_1, b_2) = \left\{ \theta(b_1 - b_2) K_0(i\sqrt{x_2 x_3} b_1 M_B) I_0(i\sqrt{x_2 x_3} b_2 M_B) + (b_1 \leftrightarrow b_2) \right\} \cdot \frac{\pi i}{2} H_0^{(1)}(\sqrt{x_1 + x_2 + x_3 - x_1 x_3 - x_2 x_3} b_1 M_B), \quad (\text{B4})$$

$$h_f^4(x_1, x_2, x_3, b_1, b_2) = \left\{ \theta(b_1 - b_2) K_0(i\sqrt{x_2 x_3} b_1 M_B) I_0(i\sqrt{x_2 x_3} b_2 M_B) + (b_1 \leftrightarrow b_2) \right\} \cdot \left(\begin{array}{ll} K_0(M_B F_{(1)} b_1), & \text{for } F_{(1)}^2 > 0 \\ \frac{\pi i}{2} H_0^{(1)}(M_B \sqrt{|F_{(1)}^2|} b_1), & \text{for } F_{(1)}^2 < 0 \end{array} \right), \quad (\text{B5})$$

where $j=1$ and 2 , J_0 is the Bessel function and K_0 , I_0 are modified Bessel functions $K_0(-ix) = -(\pi/2)Y_0(x) + i(\pi/2)J_0(x)$, and $F_{(1)}^2$, $D_{(j)}$'s are defined by

$$\begin{aligned} F_{(1)}^2 &= (x_1 - x_2)x_3, \\ D_{(1)}^2 &= (x_1 - x_2)x_3, \\ D_{(2)}^2 &= -(1 - x_1 - x_2)x_3. \end{aligned} \quad (\text{B6})$$

The threshold resummation form factor $S_t(x_i)$ is adopted from Ref.[24]

$$S_t(x) = \frac{2^{1+2c}\Gamma(3/2+c)}{\sqrt{\pi}\Gamma(1+c)} [x(1-x)]^c, \quad (\text{B7})$$

where the parameter $c = 0.3$. This function is normalized to unity.

The Sudakov factors used in the text are defined as

$$S_a(t) = s(x_1 m_B / \sqrt{2}, b_1) + s(x_3 m_B / \sqrt{2}, b_3) + s((1 - x_3) m_B / \sqrt{2}, b_3) - \frac{1}{\beta_1} \left[\ln \frac{\ln(t/\Lambda)}{-\ln(b_1 \Lambda)} + \ln \frac{\ln(t/\Lambda)}{-\ln(b_3 \Lambda)} \right], \quad (\text{B8})$$

$$S_b(t) = s(x_1 m_B / \sqrt{2}, b_1) + s(x_2 m_B / \sqrt{2}, b_2) + s((1 - x_2) m_B / \sqrt{2}, b_2) + s(x_3 m_B / \sqrt{2}, b_1) + s((1 - x_3) m_B / \sqrt{2}, b_1) - \frac{1}{\beta_1} \left[2 \ln \frac{\ln(t/\Lambda)}{-\ln(b_1 \Lambda)} + \ln \frac{\ln(t/\Lambda)}{-\ln(b_2 \Lambda)} \right], \quad (\text{B9})$$

$$S_c(t) = s(x_1 m_B / \sqrt{2}, b_1) + s(x_2 m_B / \sqrt{2}, b_2) + s((1 - x_2) m_B / \sqrt{2}, b_2) + s(x_3 m_B / \sqrt{2}, b_2) + s((1 - x_3) m_B / \sqrt{2}, b_2) - \frac{1}{\beta_1} \left[\ln \frac{\ln(t/\Lambda)}{-\ln(b_1 \Lambda)} + 2 \ln \frac{\ln(t/\Lambda)}{-\ln(b_2 \Lambda)} \right], \quad (\text{B10})$$

$$S_d(t) = s(x_2 m_B / \sqrt{2}, b_2) + s(x_3 m_B / \sqrt{2}, b_3) + s((1 - x_2) m_B / \sqrt{2}, b_2) + s((1 - x_3) m_B / \sqrt{2}, b_3) - \frac{1}{\beta_1} \left[\ln \frac{\ln(t/\Lambda)}{-\ln(b_2 \Lambda)} + \ln \frac{\ln(t/\Lambda)}{-\ln(b_3 \Lambda)} \right], \quad (\text{B11})$$

where the function $s(q, b)$ are defined in the Appendix A of Ref.[22]. The scale t_i 's in the above equations are chosen as

$$\begin{aligned}
t_e^1 &= \max(\sqrt{x_3}m_B, 1/b_1, 1/b_3) , \\
t_e^2 &= \max(\sqrt{x_1}m_B, 1/b_1, 1/b_3) , \\
t_e^3 &= \max(\sqrt{x_3}m_B, 1/b_2, 1/b_3) , \\
t_e^4 &= \max(\sqrt{x_2}m_B, 1/b_2, 1/b_3) , \\
t_f^1 &= \max(\sqrt{x_1x_3}m_B, \sqrt{(x_1 - x_2)x_3}m_B, 1/b_1, 1/b_2) , \\
t_f^2 &= \max(\sqrt{x_1x_3}m_B, \sqrt{(1 - x_1 - x_2)x_3}m_B, 1/b_1, 1/b_2) , \\
t_f^3 &= \max(\sqrt{x_1 + x_2 + x_3 - x_1x_3 - x_2x_3}m_B, \sqrt{x_2x_3}m_B, 1/b_1, 1/b_2) , \\
t_f^4 &= \max(\sqrt{(x_1 - x_2)x_3}m_B, \sqrt{x_2x_3}m_B, 1/b_1, 1/b_2) .
\end{aligned} \tag{B12}$$

-
- [1] M. Wirbel, B. Stech and M. Bauer, Z. Phys. C **29**, 637 (1985); M. Bauer, B. Stech and M. Wirbel, Z. Phys. C **34**, 103 (1987).
- [2] A. Ali, G. Kramer and C.D. Lü, Phys. Rev. D **58**, 094009 (1998); *ibid.* **59**, 014005 (1999);
- [3] D.S. Du, H.J. Gong, J.F. Sun, D.S. Yang, and G.H. Zhu, Phys. Rev. D **65**, 094025 (2002).
- [4] M. Beneke and M. Neubert, Nucl. Phys. B **675**, 333 (2003).
- [5] G.P. Lepage and S. Brodsky, Phys. Rev. D **22**, 2157 (1980); J. Botts and G. Sterman, Nucl. Phys. B **325**, 62 (1989).
- [6] H.N. Li and H.L. Yu, Phys. Rev. Lett. **74**, 4388 (1995); Phys. Rev. D **53**, 2480 (1996); T.-W. Yeh and H.N. Li, Phys. Rev. D **56**, 1615 (1997).
- [7] Y. Y. Keum, H.N. Li and A. I. Sanda, Phys. Lett. B **504**, 6(2001); Phys. Rev. D **63**, 054008 (2001).
- [8] H.N. Li, Prog.Part.& Nucl.Phys. **51**, 85 (2003), and reference therein.
- [9] C.W. Bauer, S. Fleming, and M. Luke, Phys. Rev. D **63**, 014006(2001); C.W. Bauer, S. Fleming, D. Pirjol, and I.W. Stewart, Phys. Rev. D **63**, 114020(2001); C.W. Bauer and I.W. Stewart, Phys. Lett. B **516** 134 (2001); C.W. Bauer, D. Pirjol, and I.W. Stewart, Phys. Rev. D **65** 054022 (2002).
- [10] S. Catani, M. Ciafaloni and F. Hautmann, Phys. Lett. B **242**, 97 (1990); Nucl. Phys. B **366**, 135 (1991); J.C. Collins and R.K. Ellis, Nucl. Phys. B **360**, 3 (1991).
- [11] G. Sterman, An Introduction to Quantum Field Theory, Cambridge University Press, 1993.
- [12] H.N. Li, Phys. Rev. D **66**, 094010 (2002); H.N. Li and K. Ukai, Phys. Lett. B **555**, 197 (2003).
- [13] M. Beneke, G. Buchalla, M. Neubert and C.T. Sachrajda, Nucl. Phys. B **606**, 245(2001).
- [14] H.S. Wang, X. Liu, Z.J. Xiao, L.B. Guo, and C.D. Lü, Nucl. Phys. B **738**, 243 (2006); X. Liu, H.S. Wang, Z.J. Xiao, L.B. Guo, and C.D. Lü, Phys. Rev. D **73**, 074002 (2006).
- [15] C.H. Chen and H.N. Li, Phys. Rev. D **63**, 014003 (2000).
- [16] J. Zhu, Y.L. Shen and C.D. Lü, Phys. Rev. D **72**, 054015 (2005); C.D. Lü, Y.L. Shen and W. Wang, Phys. Rev. D **73**, 034005 (2006).
- [17] BaBar Collaboration, B. Aubert *et al.*, Phys. Rev. D **74**, 072008 (2006).
- [18] Particle Data Group, W.-M. Yao *et al.*, J. Phys. G **33**, 1 (2006).

- [19] E. Barberio *et al.*, (Heavy Flavor Averaging Group), hep-ex/0603003; for update see the web page: <http://www.slac.stanford.edu/xorg/hfag>.
- [20] H.N. Li and B. Tseng, Phys. Rev. D **57**, 443 (1998).
- [21] G. Buchalla, A.J. Buras, M.E. Lautenbacher, Rev. Mod. Phys. **68**, 1125 (1996).
- [22] C.D. Lü, K. Ukai and M.Z. Yang, Phys. Rev. D **63**, 074009 (2001).
- [23] A.G. Grozin and M. Neubert, Phys. Rev. D **55**, 272 (1997); M. Beneke and Th. Feldmann, Nucl. Phys. B **592**, 3 (2001); M. Beneke, G. Buchalla, M. Neubert and C.T. Sachrajda, Phys. Rev. Lett. **83**, 1914 (1999); Nucl. Phys. B **591**, 313 (2000).
- [24] T. Kurimoto, H.N. Li, and A.I. Sanda, Phys. Rev. D **65**, 014007 (2002).
- [25] V.M. Braun and I.E. Filyanov, Z. Phys. C **48**, 239(1990).
- [26] P. Ball, J. High Energy Phys. 9809, 005 (1998); *ibid* , 9901, 010 (1999).
- [27] P. Ball, V.M. Braun, Y. Koike, and K. Tanaka, Nucl. Phys. B **529**, 323 (1998).
- [28] P. Ball and R. Zwicky, Phys. Rev. D **71**, 014015 (2005); *ibid* **71**, 014029 (2005).
- [29] C.D. Lü and M.Z. Yang, Eur. Phys. J. C **23**, 275 (2002).
- [30] J.D. Bjorken, Nucl. Phys. B (Proc. Suppl.) **11**, 325 (1989).